



Title	Stereomutation and Chemical Transformation of Organic Molecules by Light
Author(s)	張, 照明
Citation	北海道大学. 博士(理学) 甲第13674号
Issue Date	2019-03-25
DOI	10.14943/doctoral.k13674
Doc URL	http://hdl.handle.net/2115/91506
Type	theses (doctoral)
File Information	Zhang_Zhaoming.pdf



[Instructions for use](#)

Doctoral Thesis

**Stereomutation and Chemical Transformation
of Organic Molecules by Light**

(光による有機分子の立体構造転移および化
学構造変換)

Zhaoming Zhang (張 照明)

Macromolecular Science Research Division
Institute for Catalysis
Hokkaido University

Table of Contents

Chapter 1. General Introduction	1
Chapter 2. Photo Racemization and Polymerization of (R)-1,1'-Bi(2-naphthol)	17
Chapter 3. Chirality Induction to Star-Shaped Oligomers	30
Chapter 4. General Conclusions.	64
Acknowledgement	65

Chapter 1. General Introduction

1.1 Background

Chirality has a close relation with life in nature. It has been proved that the basic ingredients of organisms are basically optically active. For example, the 20 kinds of amino acids (except for glycine) which are the fundamental units of proteins in life have L-conformation whereas as the essential elements to construct RNA and DNA, nucleic acids are composed by right-handed sugars.¹ Besides, metabolic intermediates, lipids and many other biomolecules are also chiral. Hence, homochirality of biomolecules is considered responsible for the origin of life, and also crucial to sustain the activity of life. Chemists have been challenged to develop new artificial substances not only to mimic biological helices and functions but also for their potential applications in materials including chiral recognition,² asymmetric catalysis,³ optical non-linearity,⁴ chiroptical switch⁵ and circularly polarized luminescence.⁶

Optically active compounds and polymers have been so far prepared based on chiral molecules as chiral source, and the chirality information is transferred from chiral source molecules to the target molecules through intermolecular interactions. Chiral source molecules act as versatile roles in their corresponding reactions, for example, general chiral molecules are synthesized by catalytic reaction using chiral ligand;⁷ Yashima *et al.* reported that using chiral molecules as guest molecules to interact with achiral conjugated polymers led to the polymers with helical conformation;⁸ Akagi *et al.* prepared asymmetric reaction field by using liquid crystal mixture and chiral dopant, and the polymerization in this solution resulted in helical polymers.⁹

Another important source of chirality is circularly polarized light (CPL) which has been seen as a possible origin of chirality in biomolecules. Generally, sunlight and the light emitted by Hg or Xe lamp are called non-polarized light (NPL) which is a

mixture of linearly polarized light (LPL) and vibrates in all directions without any bias. Based on NPL, LPL can be obtained by linear polarizer. Light vector of single LPL always vibrates in one direction (one plane) and its intensity varies with the phase. Further modulating the LPL with a Fresnel Rhom or a $\lambda/4$ plate, it become a single-handed CPL. CPL is a “homochiral light” whose vibration direction is regularly changing but the intensity is constant.

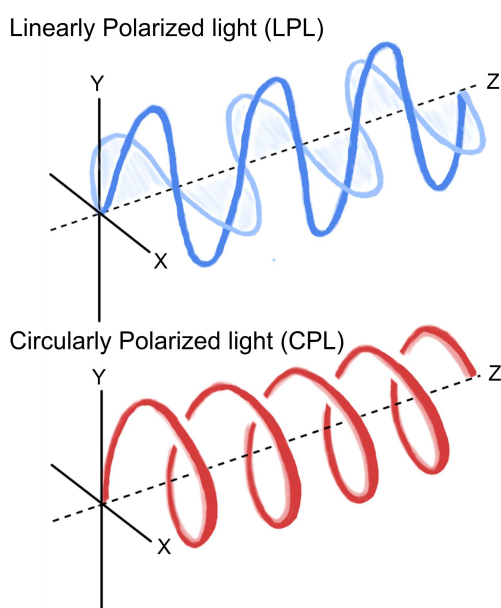


Figure. 1 linearly polarized light (LPL) and circularly polarized light (LPL).
(Dr. Yue Wang PhD Thesis, Hokkaido University)

Photochemistry is used to describe a chemical reaction caused by absorption of light. Normal photochemistry reactions give a 1:1 mixture of the enantiomers, called the racemic mixture. Moreover, pure enantiomers are thermodynamically unstable and easily to be racemized by heat or light irradiation. Asymmetric photochemistry are photoreactions by which new optical activity is created (asymmetric induction). Asymmetry in the reaction can be induced by irradiation of intense CPL. Compared with racemization driven by entropy, photo resolution requires a more extreme condition. It can be only successful if the enantiomers have a high activation energy of interconversion.

In this chapter, the background of light induced twisted-coplanar transition of

biphenyl is firstly introduced, and then the modulation of molecules and polymers conformation by using CPL are presented.

1.2 Photo-Induced Twisted-Coplanar Transition of Biphenyl

Biphenyl is a representative diaryl compound whose two aromatic rings are coupled by carbon-carbon single bond. In ground state, biphenyl adapts a twisted conformation. The twisted angle of the two rings in biphenyl has been estimated from theoretical calculations to experimentally measurements.¹⁰ The results shown that the twisted angle of biphenyl is around 45° in gas phase and 20° in solution. The twisted angle is decided by the dedicate balance of two factors: one is the repulsion of the ortho hydrogens which supports the two rings in a 90° angle; the other one is the π -electron delocalization effect and it favors a coplanar arrangement.

Biphenyl is a non-rigid molecule and is easily to undergoes a large conformational change upon excitation. Calculation reported by Hoffmann *et al.* found that in excited state biphenyl has a planar conformation. This conclusion was also verified by other papers.¹¹ It proved that in excited state, the interactions between the two phenyl rings is very strong. In this case, it is inappropriate to consider biphenyl as a dimer of benzene. Rather, the two phenyl rings can be seen as a whole with a planar conformation. Besides, the single carbon-carbon bond in biphenyl become shorter in its excited state, then the valence structure for the excited state was proposed as shown in **Scheme 1**. It is obvious that this structure favors the planar conformation of the excited biphenyl. Other report also revealed that compared with ground state, the torsional angle change for lowest singlet state is much greater than that of lowest triplet state. Therefore, it is possible that the biphenyl molecule is planar in lowest excited singlet state but a nearly planar conformation in lowest singlet state.^{11b} The twisted-coplanar transition of biphenyl can be described as in **Scheme 1**.

compounds and polymers with good photoresolution performance were gradually reported. Based on their structure, the reported cases can be divided into the following categories:

1.3.1 Bicycloketone

For CPL induced enantiomerization, successful resolution of molecules requires the simultaneous satisfaction of three factors. First, irradiation should lead to only interconversion of enantiomers and no other chemical reaction occurs. Second, the CD intensity of the enantiomers have to be sufficiently strong. Because according to the equation of $\gamma_{PSS} = g_{\lambda}/2$, degree of enantiomeric excess (e.e.) at photostationary state (γ_{PSS}) is decided by Kuhn anisotropy¹⁷ (which defined as $g_{CD} = 2(\epsilon_L - \epsilon_R)/(\epsilon_L + \epsilon_R)$, where ϵ_L and ϵ_R are molar absorptivities toward left-handed and right-handed CPLs). Third, the quantum efficiency for photoracemization must be large. Unfortunately, the g_{λ} values for organic chromophores are generally very low with the values around 10^{-4} , thus photoresolution to most of the organic compounds are undetectable. To solve this problem, Schuster and co-workers developed a series of bicycloketone whose g_{λ} values were improved by the introduction of ketone group.

Compounds **1** in **Figure 2** is the first series of bicyclic ketone in which ketone was connected on the relatively rigid bicyclo[3.3.0]octane skeleton.¹⁸ CPL irradiation on racemic mixture of these compounds in solution resulted in partial resolution with e.e. $\approx 0.4\%$. Then they developed a new skeleton of bicyclo[3.2.1]octane to build the bicyclic ketone (compound **2** in **Figure 2**).¹⁹ Through CPL irradiation on racemic mixture, e.e. at photostationary state reached a relative high level with a value of 2.5%. Using this skeleton, they further synthesized acrylic ester-substituted bicyclic ketone of compound **3**.²⁰ Though the e.e. value of compound **3** at photostationary was 0.8% which is not as high as that of compound **2**, its structure support that it is a good dopant for liquid crystalline material to modulate the phase of the materials by CPL irradiation.

The bicyclic ketone has also been incorporated in block polyisocyanates as side

chain through different linkage patterns (polymers **I**, **II**, and **III** in **Figure 2**).²¹ In order to study the influence of substituents on chiroptical properties of ketone, CPL resolution on model compounds **4**, **5**, and **6** were firstly examined to mimic the effect of the linker group on the polymers, and the e.e. were 1.7%, 1.2% and 0.97% for **4**, **5**, and **6**, respectively. Before CPL irradiation, the pendant groups on polymers are racemic, and both helical senses of the polyisocyanate backbone are equally populated. Irradiation on the pendant ketone groups with CPL resulted in not only their partial photoresolution but also the polymer backbone helix. In this process, the majority rule effect transfers the chirality of the pendant groups to the backbone of the polymers, leading to amplification of the photoresolution.

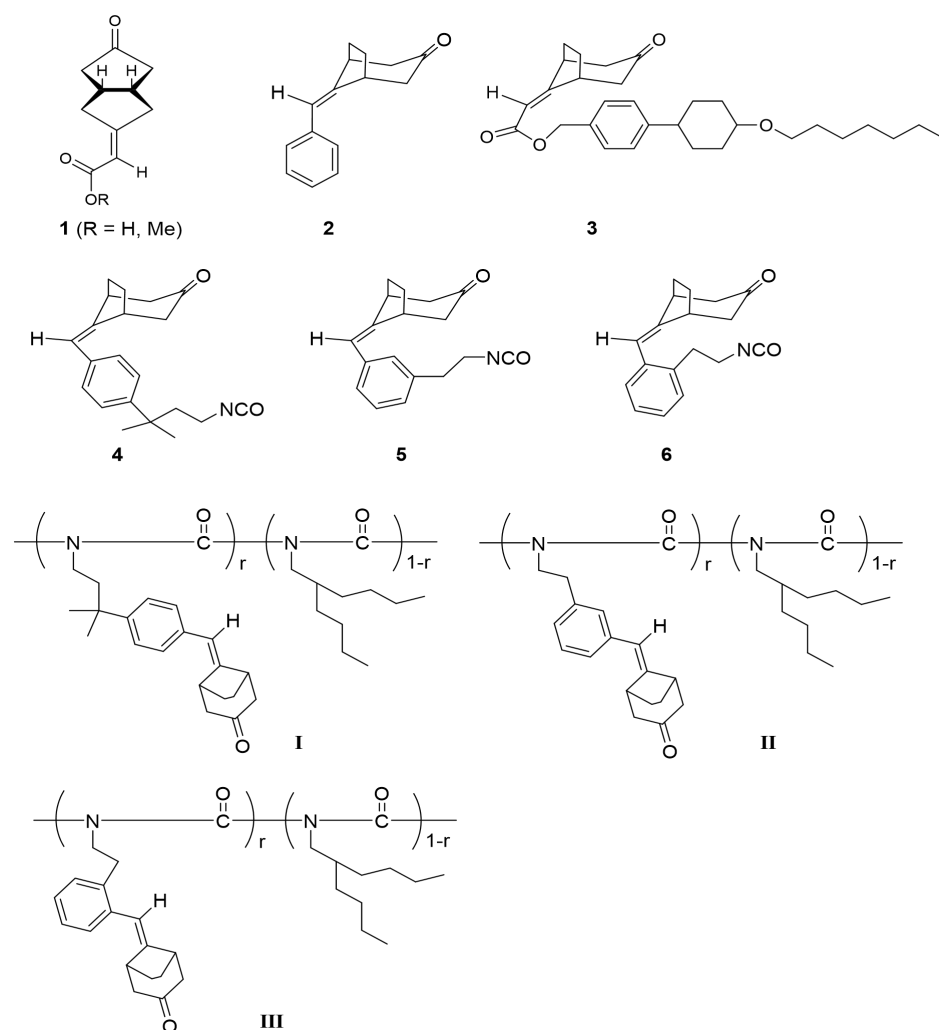


Figure 2. Chemical structures of bicycloketone molecules and polymers containing bicycloketone.

1.3.2 Overcrowded Alkene

Overcrowded alkenes are famous for their novel application as molecular motors, in which the molecular switches were generally realized by irradiation of light with different wavelength. Feringa and co-workers found that the molecular switches of one overcrowded alkene (shown in **Figure 3**) also can be controlled by irradiation of L- and R-CPL with same wavelength.²² Solution of the racemic compound irradiated by CPL led to obvious CD signals, and e.e. of the photoreaction was evaluated with a value of 0.07% at photostationary state. This photochemical interconversion is entirely reproducible and fatigue resistant. In addition, the bistable compound can be utilized as dopant in a nematic liquid crystalline phase, and the photoresolution of the compound by CPL irradiation can promote the formation of chiral mesoscopic phase.

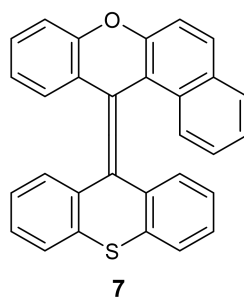


Figure 3. Chemical structure of overcrowded alkene.

1.3.3 Azobenzene and Its Derivatives.

Azobenzene is intriguing molecule whose structure can be switched between *trans* and *cis* by the irradiation of light with different wavelength. Tamaoki and co-workers reported that CPL irradiation of compounds containing azobenzene moieties led to a partially enantiomer enrichment. **8** and **9** in **Figure 4** are bicyclic and monocyclic azobenzene compounds which have planar chirality.²³ A ground state of the *cis* form of these two compounds was used as a common fast racemizing state based on which the enantiomers of the *trans* form were selectively photoisomerized by CPL. The induced e.e. for compounds **8** and **9** were 1.1% and 0.3%, respectively. After that, they further reported the CPL induced *enantio*-differentiating photoisomerization of

compound **10** with a e.e. value of 0.4%.²⁴ It is noteworthy that unlike compounds **8** and **9** having planar chirality, generation of chirality and e.e. upon CPL irradiation was from a nonchiral structure of compound **10**.

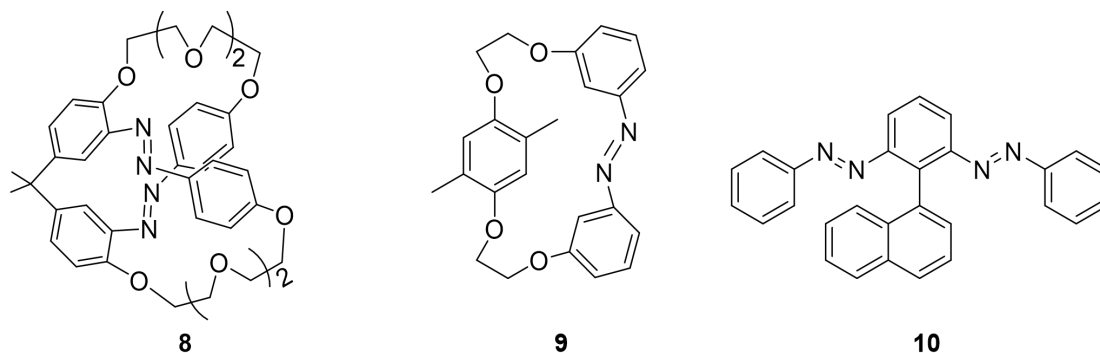


Figure 4. chemical structure of compounds containing azobenzene moieties.

CPL induced chirality of polymers containing azobenzene moieties were investigated more widely. Nikolova *et al.* firstly reported that film of polyester bearing azobenzene mesogens (polymer **IV**) exhibited strong CD signal through CPL irradiation.²⁵ After that, numerous polymers with azobenzene chromophore in their side chain were induced into optically active by using CPL as a chiral source (polymers **V-VIII** in **Figure 5**).²⁶ The induction of these polymers were conducted based on the films with liquid-crystalline or amorphous phase. In these cases, Individual azobenzene moieties is not necessary to be chiral. the CD signals induced by CPL irradiation came from the supramolecular helix which was formed by the arrangement of azobenzene moieties in the side chain.

Chirality induction was also achieved by using CPL irradiation for polyazourea with azobenzene moieties in its main chains (polymer **IX**).²⁷ Different from the polymer with azobenzene units in their side chain, the CD signal in this polymer originated from the individual chirality of the azobenzene moieties in the main-chain backbone. Fujiki *et al.* reported a CPL chirality induction of fluorene-alt-azobenzene (**X**) main chain copolymer, which was carried out based on particles state of the polymer.²⁸ CPL in this process can brake the balance of the P- and M-conformation, leading to the chirality of the particles.

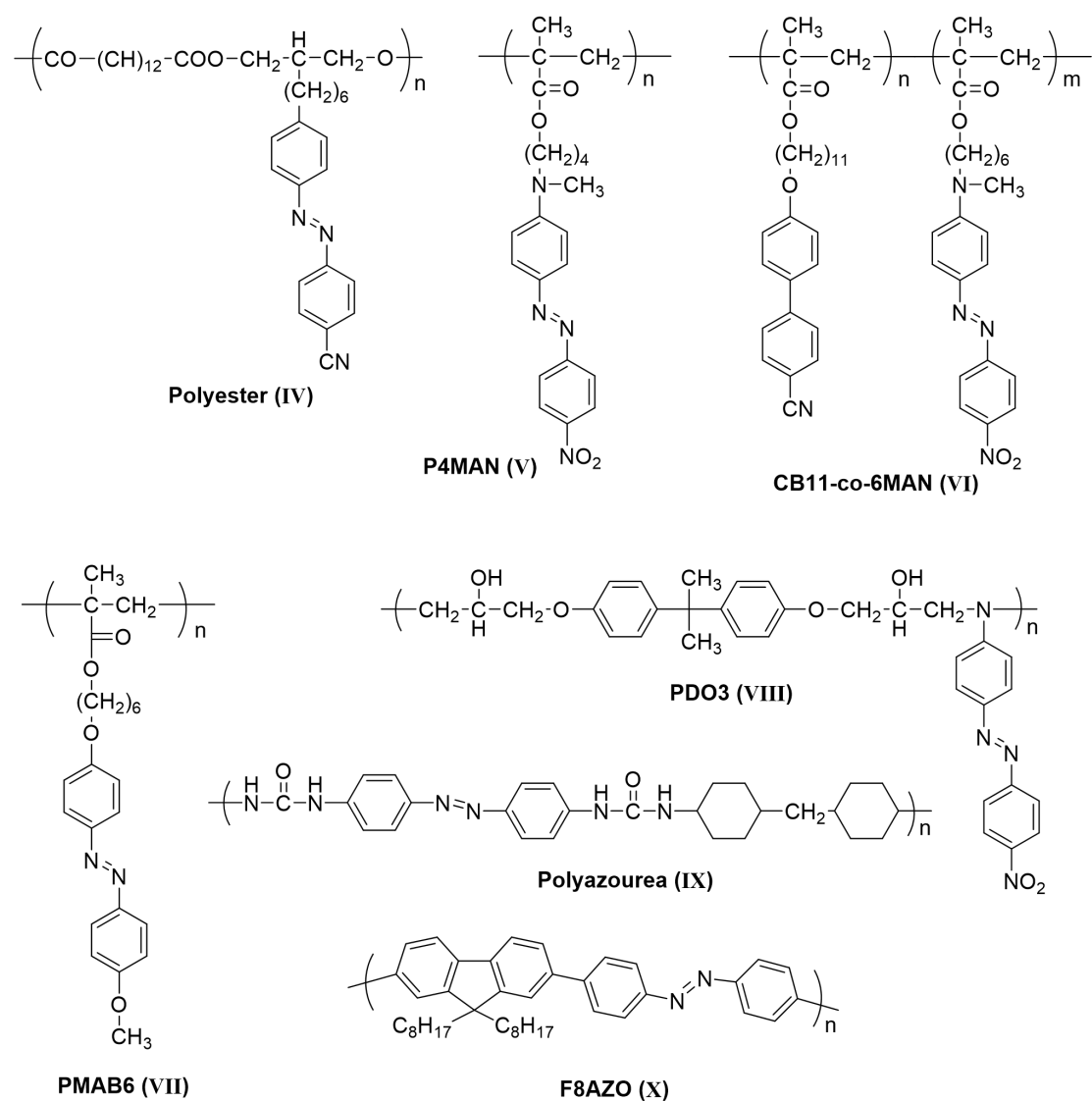


Figure 5. chemical structure of polymers containing azobenzene moieties.

1.3.4 Polyfluorene Derivatives and Oligofluorene

Our group discovered the chirality induction to conjugated polyfluorene derivatives such as PDOF (**Figure 6**) by CPL irradiation.²⁹ There is no centers or planes of chirality in the polymer structure but it has axes of chirality which coincide with the single bonds connecting the fluorene-2,7-diyl units in the main chain. The induced chirality for PDOF came from their preferred-handed helical structure. However, the helix can't be maintained in solution and is only stable in solid state. Different from the above mentioned molecules and polymers, PDOF does not have photochromic

moieties in its polymer structure. The key process in the induction was TCT. On excitation using CPL, one of the enantiomeric, right- and left-handed twists is preferentially excited into the coplanar conformation, and the excited coplanar conformation is then deactivated into both right- and left-handed twisted conformation. The relative population of the unpreferred twist hand thus increases to lead to an optically active system. It is noteworthy that chirality amplification also occurred during the induction, which was contributed to the high g_{CD} values. In addition, the research also found that β -phase is indispensable to the chirality induction, which indicates the important significance of intermolecular interaction in this process.

Then, the chirality induction to a star-shaped oligofluorene derivatives T3 (**Figure 6**) by employing CPL was reported.³⁰ The film made by T3 alone can't be induced into optically active due to the weak intermolecular interactions in the amorphous state. Surprisingly, the induction can be achieved by mixing fluorene into the film as aid molecule. The presence of fluorene molecules enhance intermolecular π - π stacking interactions by occupying the gaps between T3 molecules, whilst the fluorene crystalline surface may act as a scaffold to support the formation of a chiral structure of T3.

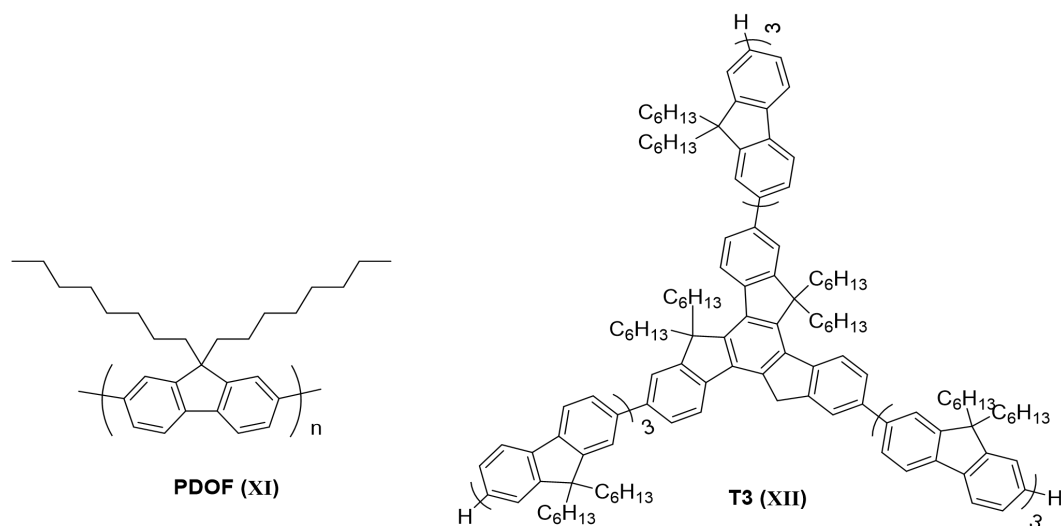


Figure 6. chemical structure of PDOF and T3.

1.4 Thesis Content

In this thesis work, NPL induced racemization of axially chiral (*R*)-1,1'-bi(2-naphthol) (BINOL) was firstly investigated to further study the “twisted-coplanar transition” theory. The irradiation of NPL led to not only racemization but also polymerization. After that, chirality induction to three star-shaped oligomers were successfully realized by CPL irradiation without using any aid molecules. The content of this thesis can be summarized as follow:

Chapter 2 presents the racemization and polymerization of (*R*)-1,1'-bi(2-naphthol) through irradiation of NPL. BINOL is a typical axially chiral molecules and it has been recognized to be stable both in chirality and chemical structure. The NPL induced racemization of BINOL indicated that the “twisted-coplanar transition” is also possible for axially chiral compounds with higher rotational barriers.³¹ Study on TCT only has been reported to for biphenyl through theoretical calculations¹¹ and experimentally established for aromatic-aromatic junctions in polymers where helical structure were induced by CPL,^{29,30} reports upon photo racemization of axially chiral compounds are rare. Besides, the irradiation of NPL also led to a polymeric product which consists not only of BINOL residues but also of residues derived from acetonitrile or reduction of BINOL.

Chapter 3 describes the CPL-based chirality induction to three star-shaped oligomers in film state with absence of aid molecules. The oligomers have no center of chirality, and the induced chiroptical properties only originated from axial chirality around the single bonds. The optically active molecules were proposed to have preferred-handed, three-blade propeller structures with three blades having the same handedness. In this work, TCT theory was applied to a new structure of N-phenylcarbazole. For two oligomers, the induced chirality was exhibited both in ground state and in excited state. In addition, the degree of induced chirality were affected by molecular aggregation and ordering in the films which played important role in the process of chirality amplification during the chirality induction.

Reference

1. (a) Crisma, M.; Toniolo, C. Helical screw-sense preferences of peptides based on chiral, C(α)-tetrasubstituted α -amino acids. *Biopolymers* **2015**, *104* (1), 46-64; (b) Travers, A.; Muskhelishvili, G. DNA structure and function. *FEBS J*, **2015**, *282* (12), 2279-2295.
2. (a) Akelah, A.; Sherrington, D. C. Application of functionalized polymers in organic synthesis. *Chem. Rev.* **1981**, *81* (6), 557-587; (b) Okamoto, Y. Separate optical isomers by chiral HPLC. *Chemtech.* **1987**, *17* (3), 177-181; (c) Okamoto, Y.; Hatada, K. Resolution of enantiomers by HPLC on optically active poly(triphenylmethyl methacrylate). *J. Liq. Chromatogr.* **1986**, *9* (2-3), 369-384; (d) Okamoto, Y.; Kaida, Y. Resolution by high-performance liquid chromatography using polysaccharide carbamates and benzoates as chiral stationary phases. *J. Chromatogr. A* **1994**, *666* (1-2), 403-419; (e) Yashima, E.; Okamoto, Y. Chiral discrimination on polysaccharides derivatives. *Bull. Chem. Soc. Jpn.* **1995**, *68* (12), 3289-3307; (f) Okamoto, Y.; Yashima, E. Polysaccharide derivatives for chromatographic separation of enantiomers. *Angew. Chem. Int. Ed.* **1998**, *37* (8), 1020-1043; (g) Yashima, E.; Yamamoto, C.; Okamoto, Y. Polysaccharide-based chiral LC columns. *Synlett* **1998**, *1998* (04), 344-360.
3. (a) Reggelin, M.; Schultz, M.; Holbach, M. Helical chiral polymers without additional stereogenic units: A new class of ligands in asymmetric catalysis. *Angew. Chem., Int. Edit.* **2002**, *41* (9), 1614-1617; (b) Muller, C. A.; Hoffart, T.; Holbach, M.; Reggelin, M. Pyridyl N-oxide substituted helically chiral poly(methacrylate)s in asymmetric organocatalysis. *Macromolecules* **2005**, *38* (13), 5375-5380; (c) Yamamoto, T.; Yamada, T.; Nagata, Y.; Suginome, M. High-molecular-weight polyquinoxaline-based helically chiral phosphine (PQXphos) as chirality-switchable, reusable, and highly enantioselective monodentate ligand in catalytic asymmetric hydrosilylation of styrenes. *J. Am. Chem. Soc.* **2010**, *132* (23), 7899-7901; (d) Yamamoto, T.; Suginome, M. Helical poly(quinoxaline-2,3-diyl)s bearing metal-binding sites as polymer-based chiral ligands for asymmetric catalysis. *Angew. Chem., Int. Edit.* **2009**, *121*(3), 547-550; (e) Reggelin, M.; Doerr, S.; Klusmann, M.; Schultz, M.; Holbach, M. Helically chiral polymers: A class of ligands for asymmetric catalysis. *Proc. Natl. Acad. Sci. U.S.A.* **2004**, *101*(15), 5461-5466; (f) Megens, R. P.; Roelfes, G. Asymmetric catalysis with helical polymers. *Chem.-Eur. J.* **2011**, *17* (31), 8514-8523; (g) Reetz, M. T.; Guo, H.; Ma, J. A.; Goddard, R.; Mynott, R. J. Helical triskelion monophosphites as ligands in asymmetric catalysis. *J. Am. Chem. Soc.* **2009**, *131* (11), 4136-4142.
4. Prasad, P. N. Polymeric materials for non-linear optics and photonics. *Polymer* **1991**, *32* (10), 1746-1751.
5. (a) Gomar-Nadal, E.; Mugica, L.; Vidal-Gancedo, J.; Casado, J.; Navarrete, J. T. L.; Veciana, J.; Rovira, C.; Amabilino, D. B. Synthesis and doping of a multifunctional tetrathiafulvalene-substituted poly(isocyanide). *Macromolecules* **2007**, *40* (21), 7521-7531; (b) Iida, H.; Mizoguchi, T.; Oh, S. D.; Yashima, E. Redox-triggered switching of helical chirality of poly(phenylacetylene)s bearing riboflavin pendants. *Polym. Chem.* **2010**, *1* (6), 841-848; (c) Hida, N.; Takei, F.; Onitsuka, K.; Shiga, K.; Asaoka, S.; Iyoda, T.; Takahashi, S. Helical,

chiral polyisocyanides bearing ferrocenyl groups as pendants: synthesis and properties. *Angew. Chem., Int. Edit.* **2003**, *115* (36), 4485-4488.

6. (a) Satrijo, A.; Meskers, S. C. J.; Swager, T. M. Probing a conjugated polymer's transfer of organization-dependent properties from solutions to films. *J. Am. Chem. Soc.* **2006**, *128* (28), 9030-9031; (b) Peeters, E.; Christiaans, M. P. T.; Janssen, R. A. J.; Schoo, H. F. M.; Dekkers, H.; Meijer, E. W. Circularly polarized electroluminescence from a polymer light-emitting diode. *J. Am. Chem. Soc.* **1997**, *119* (41), 9909-9910; (c) Kumar, J.; Nakashima, T.; Kawai, T. Circularly polarized luminescence in chiral molecules and supramolecular assemblies. *J. Phys. Chem. Lett.* **2015**, *6* (17), 3445-3452; (d) Zhang, S.; Wang, Y.; Meng, F.; Dai, C.; Cheng, Y.; Zhu, C. Circularly polarized luminescence of AIE-active chiral *O*-BODIPYs induced via intramolecular energy transfer. *Chem. Commun.* **2015**, *51* (43), 9014-9017; (e) Maeda, H. Bando, Y. Recent progress in research on stimuli-responsive circularly polarized luminescence based on π -conjugated molecules. *Pure Appl. Chem.* **2013**, *85* (10), 1967-1978.

7. (a) Noyori, R. Asymmetric catalysis: Science and opportunities (Nobel lecture). *Angew. Chem., Int. Edit.* **2002**, *41* (12), 2008-2022; (b) Satoh, K.; Kamigaito, M. Stereospecific living radical polymerization: dual control of chain length and tacticity for precision polymer synthesis. *Chem. Rev.* **2009**, *109* (11), 5120-5156.

8. (a) Liu, L.; Ousaka, N.; Horie, M.; Mamiya, F.; Yashima, E. Helix-helix inversion of an optically-inactive π -conjugated foldamer triggered by concentration changes of a single enantiomeric guest leading to a change in the helical stability. *Chem. Commun.* **2016**, *52* (79), 11752-11755; (b) Takata, L.; Iida, H.; Shimomura, K.; Hayashi, K.; dos Santos, A. A.; Yashima, E. Helical poly(phenylacetylene) bearing chiral and achiral imidazolidinone-based pendants that catalyze asymmetric reactions due to catalytically active achiral pendants assisted by macromolecular helicity. *Macromol. Rapid Commun.* **2015**, *36* (23), 2047-2054; (c) Horie, M.; Ousaka, N.; Tauraa, D.; Yashima, E. Chiral tether-mediated stabilization and helix-sense control of complementary metallo-double helices. *Chem. Sci.* **2015**, *6* (1), 714-723; (d) Qi, S.; Iida, H.; Liu, L.; Irle, S.; Hu, W.; Yashima, E. Electrical switching behavior of a [60] fullerene-based molecular wire encapsulated in a syndiotactic poly(methyl methacrylate) helical cavity. *Angew. Chem., Int. Edit.* **2013**, *52* (3), 1049-1053.

9. (a) Akagi, K.; Piao, G.; Kaneko, S.; Sakamaki, K.; Shirakawa, H.; Kyotani, M. Helical polyacetylene synthesized with a chiral nematic reaction field. *Science* **1998**, *282* (5384), 1683-1686; (b) Akagi, K.; Guo, S.; Mori, T.; Goh, M.; Piao, G.; Kyotani, M. Synthesis of helical polyacetylene in chiral nematic liquid crystals using crown ether type binaphthyl derivatives as chiral dopants. *J. Am. Chem. Soc.* **2005**, *127* (42), 14647-14654.

10. (a) Almenningen, A.; Bastiansen, O.; Fernholt, L.; Cyvin, B. N.; Cyvin, S. J.; Samdal, S. Structure and barrier of internal rotation of biphenyl derivatives in the gaseous state: Part 1. The molecular structure and normal coordinate analysis of normal biphenyl and perdeuterated biphenyl. *J. Mol. Struct.* **1985**, *128* (1-3), 59-76; (b) Bastiansen, O.; Samdal, S. Structure and barrier of internal rotation of biphenyl derivatives in the gaseous state: Part 4. barrier of internal rotation in biphenyl, perdeuterated biphenyl and seven non-ortho-substituted halogen derivatives. *J. Mol. Struct.* **1985**, *128* (1-3), 115-125; (c) Suzuki, H. Relations between electronic absorption spectra and spatial configurations of conjugated systems. I. Biphenyl. *Bull. Chem. Soc. Jpn.* **1959**, *32* (12), 1340-1350; (d) Eaton,

- V. J.; Steele, D. Dihedral angle of biphenyl in solution and the molecular force field. *J. Chem. Soc., Faraday Trans 2*. **1973**, *69*, 1601-1608; (e) Akiyama, M.; Watanabe, T.; Kakihana, M. Internal rotation of biphenyl in solution studied by IR and NMR spectra. *J. Phys. Chem.* **1986**, *90* (9), 1752-1755; (f) Roberts R. M. G. Conformational analysis of biphenyls using ^{13}C NMR spectroscopy. *Magn. Reson. Chem.* **1985**, *23* (1), 52-54.
11. (a) Im, H. S.; Bernstein, E. R. Geometry and torsional motion of biphenyl in the ground and first excited singlet state. *J. Chem. Phys.* **1988**, *88* (12), 7337-7347; (b) Lim, E. C.; Li, Y. H. Luminescence of biphenyl and geometry of the molecule in excited electronic states. *J. Chem. Phys.* **1970**, *52* (12), 6416-6422.
12. (a) Buchardt, O. Photochemistry with circularly polarized light. *Angew. Chem., Int. Edit.* **1974**, *13* (3), 179-185; (b) Bernstein, W. J.; Calvin, M.; Buchardt, O. Absolute asymmetric synthesis. I. Mechanism of the photochemical synthesis of nonracemic helicenes with circularly polarized light. Wavelength dependence of the optical yield of octahelicene. *J. Am. Chem. Soc.* **1972**, *94* (2), 494-498; (c) Bernstein, W. J.; Calvin, M.; Buchardt, O. Absolute asymmetric synthesis. II. (1) on the mechanism of the synthesis of nonracemic helicenes with circularly polarized light. Structural effects. *Tetrahedron Lett.* **1972**, *13* (22), 2195-2198; (d) Bernstein, W. J.; Calvin, M.; Buchardt, O. Absolute asymmetric synthesis. III. Hindered rotation about aryl-ethylene bonds in the excited states of diaryl ethylenes. Structural effects on the asymmetric synthesis of 2- and 4-substituted hexahelicenes. *J. Am. Chem. Soc.* **1973**, *95* (2), 527-532.
13. (a) Manaka, T.; Kon, H.; Ohshima, Y.; Zou, G.; Iwamoto, M. Preparation of chiral polydiacetylene film from achiral monomers using circularly polarized light. *Chem. Lett.* **2006**, *35* (9), 1028-1029; (b) Xu, Y.; Jiang, H.; Zhang, Q.; Wang, F.; Zou, G. Helical polydiacetylene prepared in the liquid crystal phase using circular polarized ultraviolet light. *Chem. Commun.* **2014**, *50* (3), 365-367; (c) Yang, G.; Zhu, L.; Hu, J.; Xia, H.; Qiu, D.; Zhang, Q.; Zhang, D.; Zou, G. Near-infrared circularly polarized light triggered enantioselective photopolymerization by using upconversion nanophosphors. *Chem.-Eur. J.* **2017**, *23* (33), 8032-8038.
14. (a) Blume, R.; Rau, H.; Schuster, O. Molar ellipticity of the pure enantiomer by partial photoresolution. Photoreaction of 4, 4, 4', 4'-tetramethyl-2, 2, 3', 3'-tetraazaspiro [4.4] nona-2, 2'-diene. *J. Am. Chem. Soc.* **1976**, *98* (21), 6583-6586; (b) Hörmann, M.; Ufermann, D.; Schneider, M. P.; Rau, H. Asymmetric photochemistry: transfer of optical activity from educt to product in the photolysis of trans-3,5-diphenylpyrazoline with circularly polarized light. *J. Photochem.* **1981**, *15* (3), 259-262; (c) Zimmerman, H. E.; Little, R. D. Novel photochemical 1, 4-phenyl migration. Role of the second π bond in the di- π -methane rearrangement. Mechanistic and exploratory organic photochemistry. *J. Am. Chem. Soc.* **1974**, *96* (16), 5143-5152; (d) Nelander, B.; Nordén, B. Optically active low-temperature inversion stabilised 1, 2-dithiane by photolysis with circularly polarised light. *Chem. Phys. Lett.* **1974**, *28* (3), 384-386.
15. (a) Stevenson, K. L.; Verdick, J. F. Partial photoresolution. Preliminary studies on some oxalato complexes of chromium (III). *J. Am. Chem. Soc.* **1968**, *90* (11), 2974-2975; (b) Stevenson, K. L. Partial photoresolution. III. Tris (acetylacetonato) chromium (III) system. *J. Am. Chem. Soc.* **1972**, *94* (19), 6652-6654; (c) Nordén, B. Optical activity developed by preferential racemization of one enantiomer in racemic $\text{Cr(III)(Ox)}_3^{3-}$ induced by irradiation

- with circularly polarized light. *Acta Chem. Scand.* **1970**, *24* (1), 349-351; (d) Nordén, B. Optical activity in racemic chromium(III) tartrate solution induced by circularly polarized irradiation. *Inorg. Nucl. Chem. Lett.* **1977**, *13* (8), 355-362.
16. Radziszewski, J. G.; Downing, J. W.; Jawdosiuk, M.; Kovacic, P.; Michl, J. 4-Azahomoadamant-3-ene: Spectroscopic characterization and photoresolution of a highly reactive strained bridgehead imine. *J. Am. Chem. Soc.* **1985**, *107* (3), 594-603.
17. Kuhn, W.; Knopf, E. The preparation of optically active compounds by the aid of light. *Z Phys. Chem.* **1930**, *7*, 292-310.
18. Suarez, M.; Schuster, G. B. Photoresolution of an axially chiral bicyclo[3.3.0]octan-3-one: Phototriggers for a liquid-crystal-based optical switch. *J. Am. Chem. Soc.* **1995**, *117* (25), 6732-6738.
19. Zhang, Y.; Schuster, G. B. Photoresolution of an axially chiral bicyclo[3.2.1]octan-3-one: phototriggers for a liquid crystal-based optical switch. *J. Org. Chem.* **1995**, *60* (22), 7192-7197.
20. Burnham, K. S.; Schuster, G. B. Transfer of chirality from circularly polarized light to a bulk material property: propagation of photoresolution by a liquid crystal transition. *J. Am. Chem. Soc.* **1999**, *121* (43), 10245-10246.
21. Li, J.; Schuster, G. B.; Cheon, K. S.; Green, M. M.; Selinger, J. V. Switching a helical polymer between mirror images using circularly polarized light. *J. Am. Chem. Soc.* **2000**, *122* (11), 2603-2612.
22. Huck, N. P. M.; Jager, W. F.; de Lange, B.; Feringa, B. L. Dynamic control and amplification of molecular chirality by circular polarized light. *Science*, **1996**, *273* (5282), 1686-1688.
23. (a) Tamaoki, N.; Wada, M. Dynamic control of racemization rate through *E-Z* photoisomerization of azobenzene and subsequent partial photoresolution under circular polarized light. *J. Am. Chem. Soc.* **2006**, *128* (19), 6284-6285; (b) Hashim, P. K.; Thomas, R.; Tamaoki, N. Induction of molecular chirality by circularly polarized light in cyclic azobenzene with a photoswitchable benzene rotor. *Chem.-Eur. J.* **2011**, *17* (26), 7304-7312.
24. Rijeesh, K.; Hashim, P. K.; Noro, S. I.; Tamaoki, N. Dynamic induction of enantiomeric excess from a prochiral azobenzene dimer under circularly polarized light. *Chem. Sci.* **2015**, *6* (2), 973-980.
25. Nikolova, L.; Nedelchev, L.; Todorov, T.; Petrova, T.; Tomova, N.; Dragostinova, V.; Ramanujam, P. S.; Hvilsted, S. Self-induced light polarization rotation in azobenzene-containing polymers. *Appl. Phys. Lett.* **2000**, *77* (5), 657-659.
26. (a) Iftime, G.; Labarthe, F. L.; Natansohn, A.; Rochon, P. Control of chirality of an azobenzene liquid crystalline polymer with circularly polarized light. *J. Am. Chem. Soc.* **2000**, *122* (51), 12646-12650; (b) Hore, D.; Wu, Y.; Natansohn, A.; Rochon, P. Investigation of circular Bragg reflection in an azo polymer with photoinduced chirality. *J. Appl. Phys.* **2003**, *94* (4), 2162-2166; (c) Wu, Y.; Natansohn, A.; Rochon, P. Photoinduced chirality in thin films of achiral polymer liquid crystals containing azobenzene chromophores. *Macromolecules*, **2004**, *37* (18), 6801-6805. (d) Kim, M. J.; Shin, B. G.; Kim, J. J.; Kim, D. Y. Photoinduced supramolecular chirality in amorphous azobenzene polymer films. *J. Am. Chem. Soc.* **2002**, *124* (14), 3504-3505.
27. Choi, S. W.; Fukuda, T.; Takanishi, Y.; Ishikawa, K.; Takezoe, H. Light-induced

macroscopic chirality in thin films of achiral main-chain amorphous polyazourea system. *Jpn. J. Appl. Phys.* **2006**, *45* (1S), 447.

28. Fujiki, M.; Yoshida, K.; Suzuki, N.; Zhang, J.; Zhang, W.; Zhu, X. Mirror symmetry breaking and restoration within μm -sized polymer particles in optofluidic media by pumping circularly polarised light. *RSC Adv.* **2013**, *3* (15), 5213-5219.

29. (a) Wang, Y.; Sakamoto, T.; Nakano, T. Molecular chirality induction to an achiral π -conjugated polymer by circularly polarized light. *Chem. Commun.* **2012**, *48* (13), 1871-1873; (b) Wang, Y.; Harada, T.; Phuong, L. Q.; Kanemitsu, Y.; Nakano, T. Helix induction to polyfluorenes using circularly polarized light: chirality amplification, phase-selective induction, and anisotropic emission. *Macromolecules* **2018**, *51* (17), 6865-6877; (c) Pietropaolo, A.; Wang, Y.; Nakano, T. Predicting the switchable screw sense in fluorene-based polymers. *Angew. Chem. Int. Ed.* **2015**, *54* (9), 2688-2692.

30. Wang, Y.; Kanibolotsky, A. L.; Skabara, P. J.; Nakano, T. Chirality induction using circularly polarized light into a branched oligofluorene derivative in the presence of an achiral aid molecule. *Chem. Comm.* **2016**, *52* (9), 1919-1922.

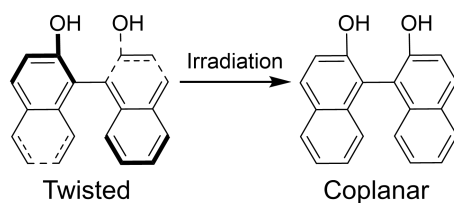
31. Zhang, Z.; Wang, Y.; Nakano, T. Photo racemization and polymerization of (*R*)-1,1'-bi (2-naphthol). *Molecules*, **2016**, *21* (11), 1541.

Chapter 2. Photo Racemization and Polymerization of (*R*)-1,1'-Bi(2-naphthol)

2.1 Introduction

Interactions between substances and light play important roles in life. Typically, sunlight acts as the deriving energy in photosynthesis for plants and other organisms where sugars and molecular oxygen are produced from carbon dioxide and water. As for artificial chemical synthesis, though so far photochemistry has not been used as an important method to industrial mass production of chemicals, it has its firm stand in laboratory because of its unique significance in synthesis, in kinetic and mechanistic work, and in the development of general concepts.¹ Further, as described in chapter 1, circularly polarized light (CPL) can prompt the photochemistry reactions to obtain non-racemic products. Our group is interested in CPL induced chirality for molecules and polymers having diaryl units connected by single bonds which is represented by PDOF. From the viewpoint of mechanism, twisted-coplanar transition (TCT) played a key role in the induction. TCT by photo excitation was firstly predicted for biphenyl through theoretical calculations. However, up to now experimental study on TCT for small molecules is rarely reported.

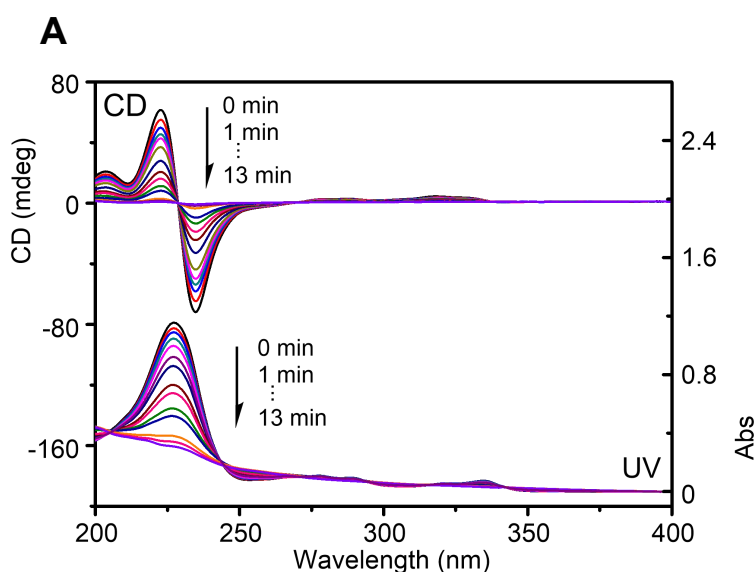
1,1'-Bi(2-naphthol) (BINOL) is a particularly compound with axial chirality. Compared with binaphthyl, the 2,2'-substituents OH in BINOL endow it resolvable as optically active enantiomers. Therefore, BINOL has been used as an effective chiral ligand and also as a building block for chiral functional molecules and polymers; its stability has been considered to be sufficient under normal conditions for organic synthesis.² In this chapter, (*R*)-1,1'-Bi(2-naphthol) was irradiated by non-polarized light (NPL) to study the TCT for a molecule with a higher rotational barrier. Upon NPL irradiation, BINOL was readily to be racemized through a TCT process (**Scheme 1**). In addition, polymerization also occurred at the same time.



Scheme 1. Twisted-coplanar transition (TCT) of BINOL.

2.2 Photo-Induced Racemization

CPL irradiation on BINOL in a solution of acetonitrile was conducted under N_2 atmosphere with light using a 500-W Hg-Xe lamp without any modulation or polarization. **Figure 1A** shows the changes of UV and circular dichroism (CD) spectra upon irradiation. Intensity of CD decreased sharply through irradiation and the signal almost completely disappeared within ca. 15 min of irradiation. Meanwhile, the irradiation of NPL also led to a large decrease of UV intensity (hypochromism). These results indicate the stereo chemical and chemical transformation of BINOL through photoexcitation. Hypochromism due to photoexcitation has been reported in the poly(9,9-di-*n*-octylfluorene-2,7-diyl) work where it was found that change in dihedral angle in the main chain was responsible for that. However, the hypochromism observed in this work seem to have a connection with polymer formation as discussed later.



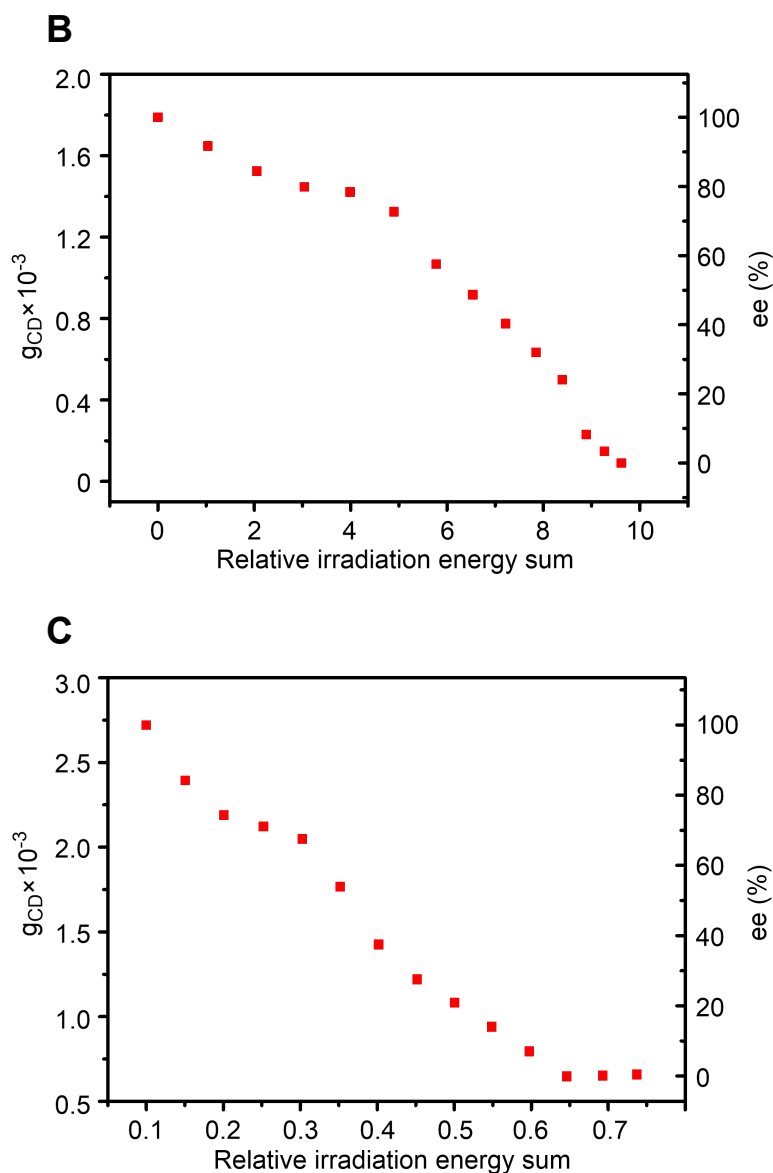


Figure 1. Changes in chirality of (*R*)-BINOL in CH₃CN solution upon irradiation ([BINOL]₀ = 1.0 × 10⁻⁴ M, cell path 1 mm, room temperature): (A) CD and UV spectra taken upon irradiation for 13 min at 1-min interval; (B) g_{CD} -vs.-relative irradiation energy plot at 223 nm; (C) g_{CD} -vs.-relative irradiation energy plot at 318 nm. Copyright (2016) MDPI.

The reason of mutarotation was further investigated by chromatographic resolution of the BINOL samples after irradiation, and the results were exhibited in **Figure 2**. The resolution was based on a Daicel Chiralpak IA column with the size of 25 cm × 0.46 cm (i.d.), flow rate was 0.5 mL/min, and eluent was a mixture of hexane and dichloromethane (50/50, v/v). As shown in **Figure 2A**, racemic BINOL can be

completely resolved with chromatographic factors, $k_1 = 2.35$ and $\alpha = 1.61$. The sample before irradiation only had one signal with a elution time of 14.9 min which is identical to the (*R*)-isomer (**Figure 2B**). While the irradiation of NPL produced a new signal located around 10.6 min which can be assigned as (*S*)-isomer, and the relative intensity of this signal increased with increasing irradiation time (**Figure 2C-E**). These results fully prove that the decrease in CD intensity was due to racemization of BINOL. Photo racemization of diaryl compounds having axial chirality including BINOL,³ a BINOL derivative,⁴ 1,1'-binaphthyl,⁵ a biphenyl derivative⁶ and a 1,1'-biphenanthrene derivative⁷ have been reported. Besides, decomposition of one BINOL enantiomer was also realized in the presence of a protein.⁸

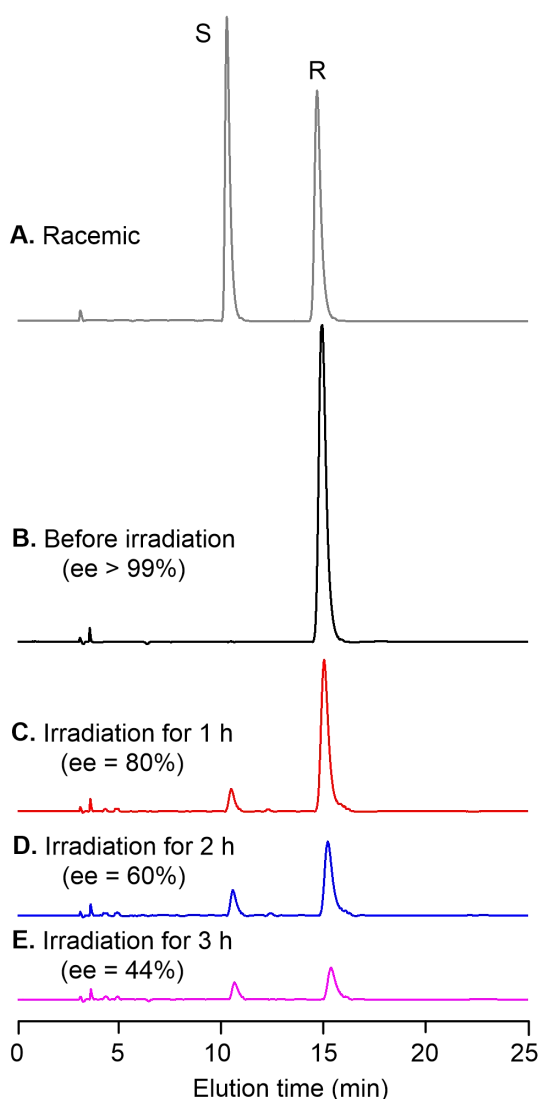


Figure 2. HPLC chromatograms of samples obtained from (*R*)-BINOL in a CH₃CN solution upon irradiation ($[(R)\text{-BINOL}]_0 = 1.00 \times 10^{-3}$ M, cell path = 5 mm, solution volume = ca. 1.75 mL) and standard samples: (A) standard racemic BINOL; (B) standard (*R*)-BINOL; (C)-(E) samples after irradiation for 1 h, 2 h, and 3 h, respectively. Copyright (2016) MDPI.

The change in chirality due to irradiation was quantitatively analyzed by evaluating chirality in terms of Kuhn's anisotropy factor (g_{CD}). Plots of g_{CD} and enantiomeric excess (e.e.) against relative irradiation energy sum (relative absorbed dose) based on the wavelength of 223 nm and 318 nm are displayed in **Figure 1B** and **C**. Because the UV intensity decreases with irradiation time, "relative irradiation energy sum"⁹ would be much suitable than irradiation time for the quantity on the horizontal axis. It equal to the sum of irradiation time intervals (Δt_i) used to change a CD spectrum to the directly following CD spectrum multiplied by UV absorbance (Abs_i) corresponding to the former CD spectrum according to the following equation:

$$\text{Relative irradiation energy sum} = \sum^n \Delta t_i \times Abs_i$$

For chiral compounds, g_{CD} is proportional to enantiomeric excess (e.e.). Hence, all the g_{CD} points in **Figure 1B** and **C** can be correlated to e.e. of BINOL based on the g_{CD} of optically pure (*R*)-BINOL before irradiation. Under the present experimental conditions where light intensity is constant, in other words, number of photons per time hitting the system is constant throughout the reaction, the rate of decrease in g_{CD} and e.e. would depend only on and is proportional to the concentration of un-racemized (*R*)-BINOL (a first-order relation) which would lead to a concave upward curve with negative slopes increasing with an increase in relative energy absorbed by the system. However, the plots of **Figure 1B** and **C** don't fit to a first-order relation, which indicates that the irradiated solution undergoes not only racemization but also another chemical transformation which affects the efficiency of photo racemization.

2.3 Photo-Induced Polymerization.

The chemical transformation of BINOL samples was studied by size-exclusion chromatography (SEC), and the profiles are shown in **Figure 3**. Before irradiation, a sharp signal of BINOL was observed at around 21.2 min. However, the irradiation of NPL resulted in an additional signals in the range of 17.6-22.6 min and the intensity of this signal increased with the with irradiation time. It is a strong evidence to prove the formation of polymers during irradiation. Though the molecular weight of the product is only less than a few hundred, the highest M_n values of the product at 17.6 min is 2,000. Up to now, it can be proposed that NPL irradiation on BINOL solution led to polymerization as well as racemization.

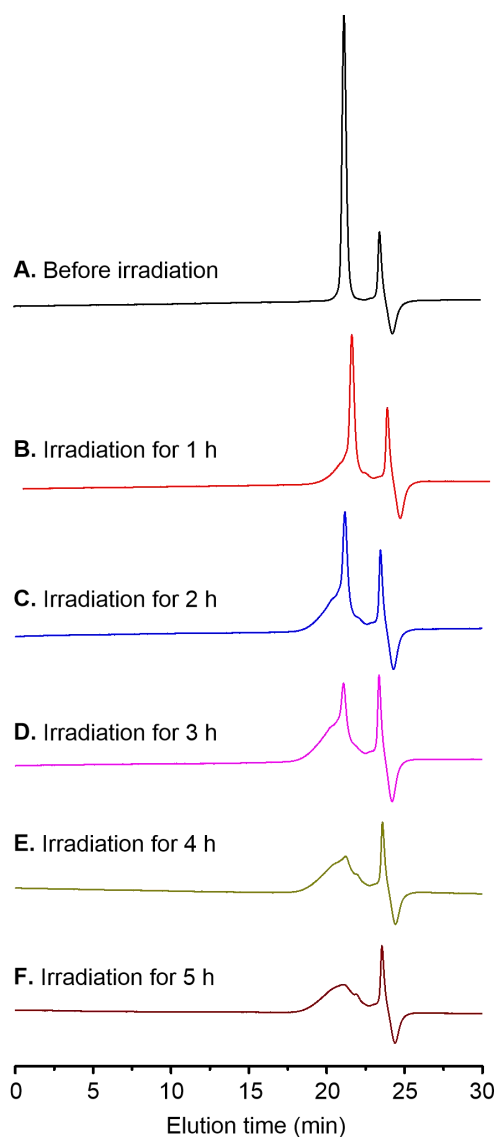


Figure 3. SEC chromatograms of samples obtained from (*R*)-BINOL in a CH₃CN solution upon irradiation ($[(R)\text{-BINOL}]_0 = 1.00 \times 10^{-3}$ M, cell path = 5 mm, solution volume = ca. 1.75 mL) and a standard (*R*)-BINOL sample: (A) standard (*R*)-BINOL; (B)-(F) samples after irradiation for 1 h, 2 h, 3 h, 4 h, and 5 h, respectively. Copyright (2016) MDPI.

Now, the deviation of e.e.-vs.-relative energy plots in **Figure 1** from a shape expected for a first-order reaction can be reasonably explained by the formation of polymer. In addition, the polymerization may be also responsible for the decreased intensity in UV spectra in **Figure 1A**.

In order to obtain information of the polymer, measurements of ¹H NMR and IR were performed with the spectra shown in Figures 4 and 5. Broad aromatic signals can be observed in **Figure 4**, which further proves the formation of polymer. Besides, rather intense signals emerged in the range of 0.8~5.33 ppm in product NMR spectra, which indicates that the polymeric product does not consist purely of BINOL units but it may have a partially reduced structure and may have residues arising not only from BINOL but also from acetonitrile, the solvent. This aspect was further assessed by IR spectra (**Figure 5**). Compared with the signals of BINOL, those of the product were much broader, which is consistent with the formation of a polymer. In addition, signals due to aromatic C-H out-of-plane bending vibration including the intense ones at 815 and 747 cm⁻¹ are much weaker in the polymer spectrum which supports the partial loss of aromaticity due to reduction. Further, rather intense signals at around 1700 cm⁻¹ can be seen in spectra of the product which would not be ascribed to a polymer consisting only of BINOL units and may be due to the C=N or C=O functions. This result suggests that acetonitrile might have a role in the photo polymerization or that C=O species which has been proposed to form upon irradiation^{3b,c} might be incorporated into polymer chain. Notably, the signals of BINOL in the range of 3000-4000 cm⁻¹ were largely broadened after irradiation, which might mean the formation of intra-molecular hydrogen-bonding between -OH groups of neighboring units in the polymeric product with various strengths and forms.

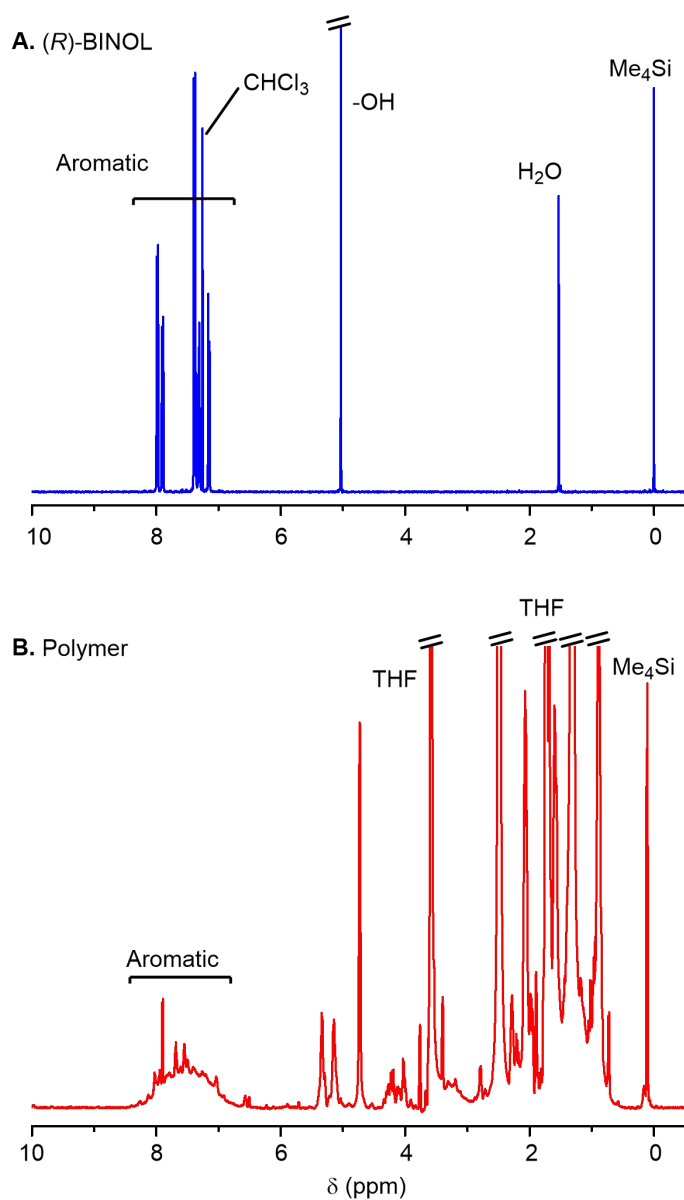


Figure 4. ^1H NMR spectra: (A) (*R*)-BINOL taken in CDCl_3 ; (B) the polymeric product obtained from (*R*)-BINOL in a CH_3CN solution upon irradiation for 5 h ($[(R)\text{-BINOL}]_0 = 1.00 \times 10^{-3}$ M, cell path = 5 mm) taken in THF-d_8 [400 MHz, room temperature, Me_4Si]. Copyright (2016) MDPI.

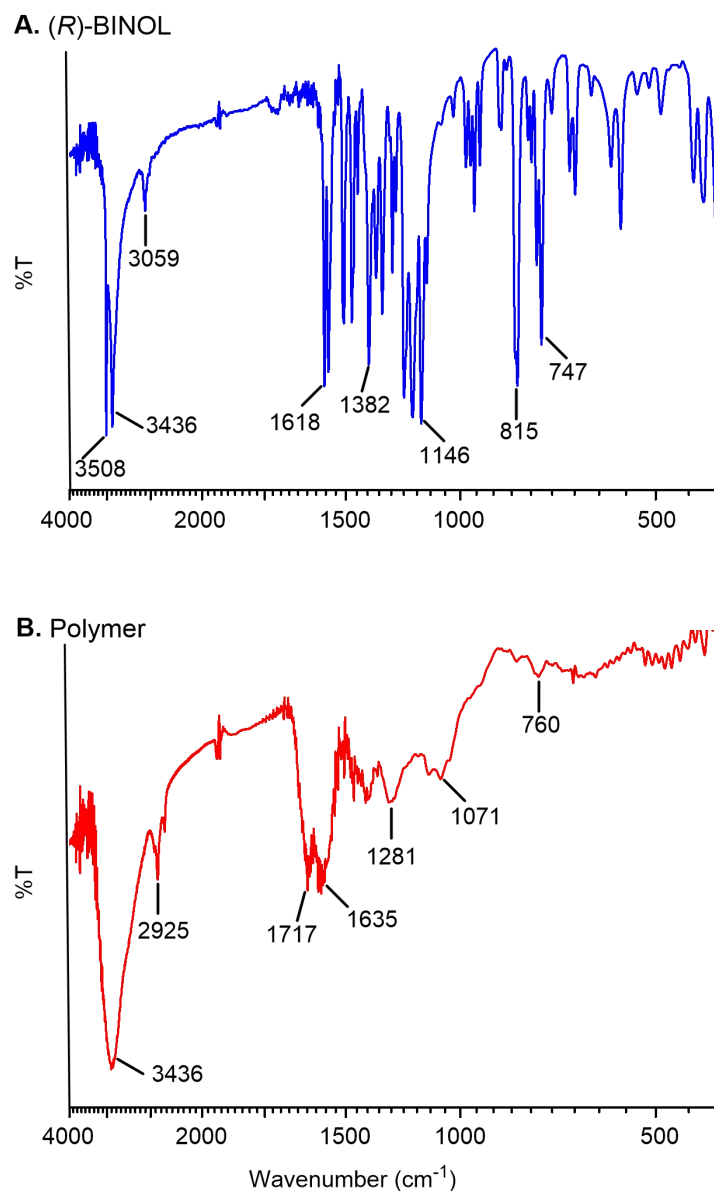


Figure 5. IR spectra: (A) (*R*)-BINOL; (B) the polymeric product obtained from (*R*)-BINOL in a CH₃CN solution upon irradiation for 5 h ($[(R)\text{-BINOL}]_0 = 1.00 \times 10^{-3}$ M, cell path = 5 mm) [KBr pellet]. Copyright (2016) MDPI.

Elemental analysis of a polymer obtained in a repeated experiment under conditions similar to those for the HPLC and SEC measurements with an irradiation time of 4 h further verified the analysis on NMR and IR spectra. If the polymer is only composed by BINOL unit, its ratio of elements would be close to the value for BINOL (C, 83.90%; H, 4.93%). However, the result obtained in experiment was C,

58.95%; H, 4.73%; N, 3.54%. These results support that the product has N atoms arising from CH₃CN and that BINOL was partially reduced on incorporation into the polymer chain.

The comparison of emission spectra for BINOL and the polymeric product was also conducted as shown in **Figure 6**. For (*R*)-BINOL, there only one sharp emission peak at around 370 nm in the spectra, while the polymeric product showed much broader emission signals. using 9,10-diphenylanthracene (0.90 in cyclohexane) as standard,¹⁰ emission efficiencies of BINOL and the polymer were measured with the values of 0.04 and 0.03, respectively. The value for BINOL well matches the one in literature.¹¹ The broader signals of the polymer may be caused by an extended π -conjugation system derived from the BINOL backbone. Changes in emission spectra of BINOL and related compounds due to their photo degradation have been reported;¹² however, polymer formation during the photo reactions have never been proposed.

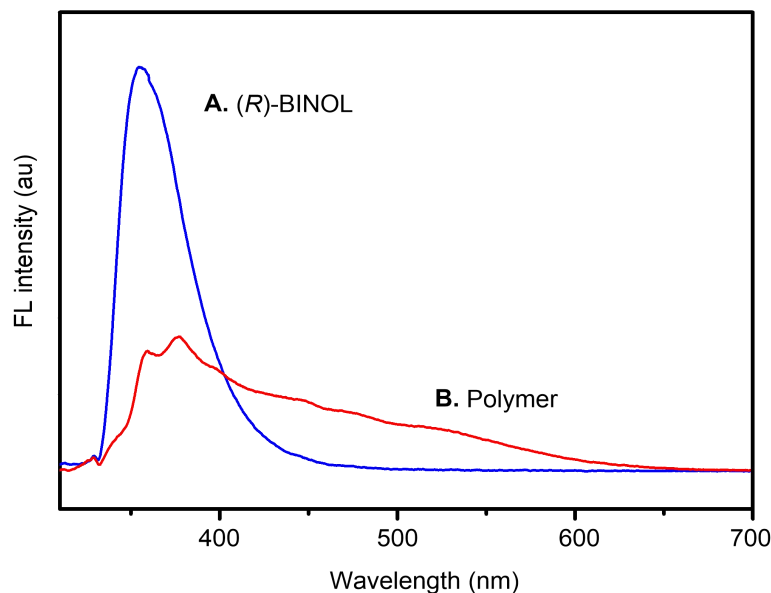


Figure 6. Emission spectra: (A) (*R*)-BINOL in a CH₃CN solution; (B) the polymeric product obtained from (*R*)-BINOL in a CH₃CN solution upon irradiation for 4.5 min ($[(R)\text{-BINOL}]_0 = 1.0 \times 10^{-6}$ M, cell path = 10 mm) [λ_{ex} 300 nm]. Intensity was normalized to a constant absorbance at 300 nm. Copyright (2016) MDPI.

2.4 Conclusions

(*R*)-BINOL was found to racemize and polymerize upon photo irradiation. The racemization may occur through TCT of BINOL on photo excitation. Although TCT has been reported to for biphenyl through theoretical calculations and experimentally established for aromatic-aromatic junctions in polymers leading to a helical structure upon irradiation using CPL, reports upon photo racemization of axially chiral compounds are rare. The finding of co-occurring photo racemization and polymerization of optically active BINOL is unprecedented while there have been only a few, related publications about photo-induced racemization of diaryl compounds. The observation in this work is in a sharp contrast to the general recognition that BINOL is a rather robust chiral backbone to be used for catalysis and for construction of chiral materials. Studies are under way to clarify the polymer structure and the mechanism of the photo racemization and polymerization as well as to find a way to make an optically active polymer from racemic BINOL with the aid of light.

2.5 Experimental

Materials. (*R*)- and racemic BINOL (Wako Chemical) and acetonitrile (Kanto Chemical) were used as purchased.

Measurements. ¹H NMR spectra were recorded on a JEOL ESC400 spectrometer (400 MHz). Size-exclusion chromatography (SEC) measurements were carried out using a chromatographic system consisting of a JASCO DG-980-50 degasser, a HITACHI L-7100 pump, a HITACHI L-7420 UV-Vis detector and a HITACHI L-7490 RI detector, equipped with TOSOH TSKgel G3000HHR and G6000HHR columns (30 × 0.72 (i.d.) cm) connected in series (eluent: THF, flow rate: 1.0 mL/min). HPLC resolution was conducted using a chromatographic system consisting of a JASCO DG-980-50 degasser, a JASCO PU-980 pump, and a JASCO UV-2070

plus UV detector (230 nm) equipped with a Daicel Chiral Pak IA column (25 cm x 0.46 cm (i.d.)) with a mixture of hexane and dichloromethane (50/50, v/v) as eluent. Circular dichroism (CD) spectra were taken with a JASCO-820 spectrometer. UV-Vis spectra were measured on JASCO V-550 and V-570 spectrophotometers. FT-IR spectra were recorded on a JASCO FT/IR-6100 spectrometer. Emission spectra were taken using a JASCO FP-8500 fluorescence spectrophotometer.

Photo irradiation. Using an Ushio Optical Modulex SXUID500MAMQQ 500-W Hg-Xe lamp under N₂ atmosphere at ambient temperature (ca. 23 °C).

References

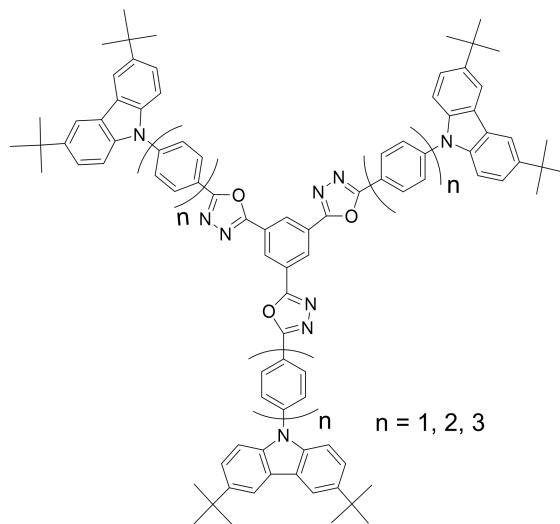
1. (a) Asandei, A. D. Photomediated controlled radical polymerization and block copolymerization of vinylidene fluoride. *Chem. Rev.* **2016**, *116* (4), 2244-2274; (b) Dadashi-Silab, S.; Doran, S.; Yagci, Y. Photoinduced electron transfer reactions for macromolecular syntheses. *Chem. Rev.* **2016**, *116* (17), 10212-10275. (c) Keukeleire, D. D.; He, S.-L. Photochemical strategies for the construction of polycyclic molecules. *Chem. Rev.* **1993**, *93* (1), 359-380; (d) Dilling, W. L. Intramolecular photochemical cycloaddition of nonconjugated olefins. *Chem. Rev.* **1966**, *66* (4), 373-393; (e) Hoffmann, N. Photochemical reactions as key steps in organic synthesis. *Chem. Rev.* **2008**, *108* (3), 1052-1103.
2. (a) Pu, L. 1,1'-Binaphthyl dimers, oligomers, and polymers: molecular recognition, asymmetric catalysis, and new materials. *Chem. Rev.* **1998**, *98* (7), 2405-2494; (b) Takata, T.; Furusho, Y.; Murakawa, K.; Endo, T.; Matsuoka, H.; Hirasa, T.; Matsuo, J.; Sisido, M. Optically active poly(aryl carbonates) consisting of axially chiral units. chiral binaphthyl group induced helical polymer. *J. Am. Chem. Soc.* **1998**, *120* (18), 4530-4531; (c) Habae, S.; Seko, T.; Okamoto, Y. Asymmetric oxidative coupling polymerization of optically active tetrahydroxybinaphthalene derivative. *Macromolecules* **2002**, *35* (7), 2437-2439.
3. (a) Cavazza, M.; Zandomenighi, M.; Ouchi, A.; Koga, Y. Photochromism in 1,1'-bi-2-naphthols. *J. Am. Chem. Soc.* **1996**, *118* (41), 9990-9991; (b) Flegel, M.; Lukeman, M.; Wan, P. Photochemistry of 1,1'-bi-2-naphthol (BINOL)-ESIPT is responsible for photoracemization and photocyclization. *Can. J. Chem.* **2008**, *86* (2), 161-169; (c) Solntsev, K. M.; Bartolo, E. A.; Pan, G.; Muller, G.; Bommireddy, S.; Huppert, D.; Tolbert, L. M. Excited-state proton transfer in chiral environments: Photoracemization of BINOLs. *Isr. J. Chem.* **2009**, *49* (2), 227-233.
4. Tetreau, C.; Lavalette, D.; Cabaret, D.; Geraghty, N.; Welvart, Z. Bridged derivatives of binaphthol- kinetic factors governing the enantiomeric stability of atropisomers in their triplet-state. *Nouv. J. Chim.* **1982**, *6* (10), 461-465.
5. Irie, M.; Yoshida, K.; Hayashi, K. Laser photolysis study of the photoracemization of 1, 1'-binaphthyl. *J. Phys. Chem.* **1977**, *81* (10), 969-972.

6. Zimmerman, H. E.; Crumrine, D. S. Duality of mechanism in photoracemization of optically active biphenyl. mechanistic and exploratory organic photochemistry. LXX. *J. Am. Chem. Soc.* **1972**, *94* (2), 498-506.
7. (a) Hattori, T.; Shimazumi, Y.; Goto, H.; Yamabe, O.; Morohashi, N.; Kawai, W.; Miyano, S. Synthesis, resolution, and absolute stereochemistry of (-)-blestriarene C. *J. Org. Chem.* **2003**, *68* (6), 2099-2108; (b) Hattori, T.; Shimazumi, Y.; Yamabe, O.; Koshiishi, E.; Miyano, S. First determination of the absolute stereochemistry of a naturally occurring 1,1'-biphenanthrene, (-)-blestriarene c, and its unexpected photoracemization. *Chem. Commun.* **2002**, (19), 2234-2235.
8. Zandomenghi, M. Photochemical activation of racemic mixtures in biological matrices. *J. Am. Chem. Soc.* **1991**, *113* (20), 7774-7775.
9. Wang, Y.; Kanibolotsky, A. L.; Skabara, P. J.; Nakano, T. Chirality induction using circularly polarized light into a branched oligofluorene derivative in the presence of an achiral aid molecule. *Chem. Commun.* **2016**, *52* (9), 1919-1922.
10. Hamai, S.; Hirayama, F. Actinometric determination of absolute fluorescence quantum yields. *J. Phys. Chem.* **1983**, *87* (1), 83-89.
11. Hassan, K.; Yamashita, K.-i.; Hirabayashi, K.; Shimizu, T.; Nakabayashi, K.; Imai, Y.; Matsumoto, T.; Yamano, A.; Sugiura, K.-i. π -Expanded axially chiral biaryls and their emissions: molecular design, syntheses, optical resolution, absolute configuration, and circularly polarized luminescence of 1,1'-bipyrene-2,2'-diols. *Chem. Lett.* **2015**, *44* (11), 1607-1609.
12. (a) He, Y.; Lv, Y.; Hu, J.; Qi, L.; Hou, X. Simple, sensitive and on-line fluorescence monitoring of photodegradation of phenol and 2-naphthol. *Luminescence* **2007**, *22* (4), 309-316; (b) Taupier, G.; Boeglin, A.; Crégut, O.; Mager, L.; Barsella, A.; Gąsior, K.; Rehspringer, J.-L.; Dorkenoo, K. D. Beating photo-degradation in sum-frequency imaging of chiral organic media. *Opt. Mater.* **2015**, *45*, 22-27.

Chapter 3. Chirality Induction to Star-Shaped Oligomers

3.1 Introduction

Reactions to produce optically active materials are essential to possess a chiral source which can transfer their chiral property to the target materials. Commonly, The chiral sources in the reactions are the chiral molecules or polymers which act as ligands or additives, and the transfers of the chirality to the products are through intermolecular interactions. For these methods, there are some limitations can not be avoided such as the high costs of chiral catalyst and additives for the reactions or the difficulties in the separation after reactions. An alternative chiral source is CPL whose chirality can be transferred to the products by irradiation. We have reported the CPL induction to polyfluorene derivatives and oligofluorene, in which TCT is the key step of chirality induction. Polymers or molecules achieved chirality induction by TCT does not need photochromic moieties like azobenzene, and are more easier to be synthesized. In this chapter, this CPL induction method on the basis of TCT has been further extended to a new series of star-shaped oligomers (**Scheme 1**) without fluorene moiety in their structure.



S1 $n = 1$, M_n 1341; **S2** $n = 2$, M_n 1569; **S3** $n = 3$, M_n 1797

Scheme 1. Structures of star-shaped oligomers (**S1**, **S2**, and **S3**)

3.2 Chirality Induction

The three star-shaped oligomers have high efficient and blue emission in solution and solid state. In addition, they also have some other advantages such as high thermal stability, good solubility and excellent film-forming properties. Therefore, they are considered to be good candidates for organic light-emitting diodes (OLEDs).¹ Although there are no chirality center in their structures, axial chirality is possible. The chirality induction to obtain optically active, preferred-handed propeller molecules is described in this chapter.

The chirality induction firstly started from the CPL irradiation on a solution of **S2** in chloroform. As shown in **Figure 1**, no detectable CD signal can be observed for the solution even the irradiation time was 6 h, and UV spectra also did not have remarkable difference after CPL irradiation. This phenomenon is normal because conformational dynamic of the molecules is extremely fast and the rotational angle and direction is random in solution. Hence, the axial chirality of these oligomers can not be induced in solution.

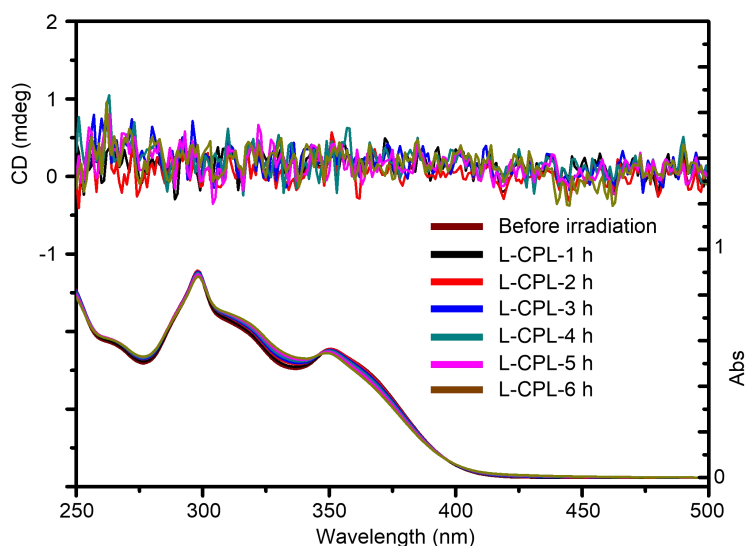


Figure 1. CD/UV spectra of **S2** in chloroform solution (concentration: 1.0×10^{-5} M) on irradiation of L-CPL.

To avoid conformational flexibility, the chirality induction to the oligomers were based on their films which were made by casting their chloroform solutions on quartz

plate. The chirality induction were performed using circularly polarized light under an nitrogen atmosphere. All the three oligomers were CD-silent when the films were casted. While irradiated by L-CPL, remarkable positive signals with Cotton band around 370, 370, and 375 nm for **S1-S3** appeared in the CD spectra as shown in **Figure 2**. What's more, the films irradiated by R-CPL led to negative CD signals which are the mirror image of those induced by L-CPL. These results prove that CPL induced a chiral conformation to the molecules.

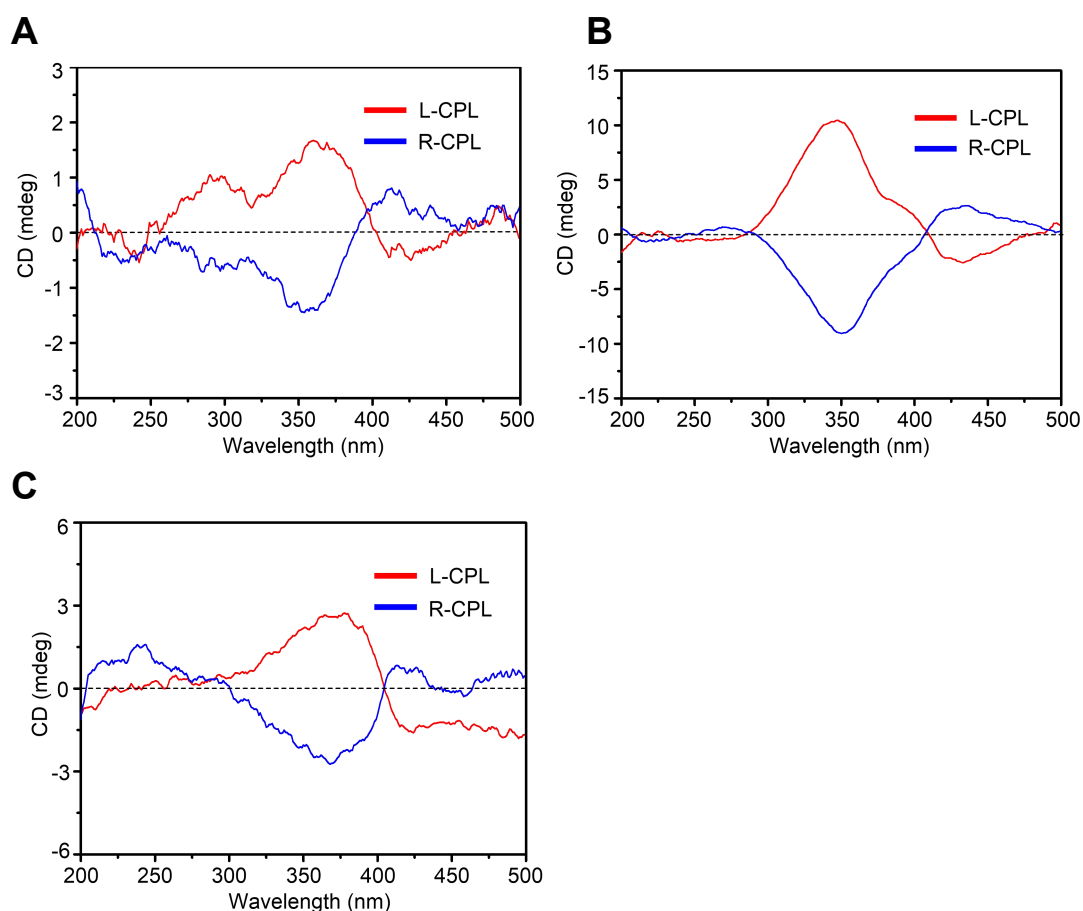


Figure 2. CD spectra induced by L- and R-CPL irradiation to **S1**, **S2**, and **S3** (A, B, and C, respectively), The films were prepared from solutions at 5.0×10^{-3} M for **S1** and **S2** and at 2.5×10^{-3} M for **S3**.

In Chapter 2, we found that NPL irradiation on binaphthol resulted in chemical transformation. Therefore, the chemical structure of these three molecules after CPL irradiation were also studied. **Figure 3** exhibits the FT-IR spectra of the molecules, and no change can be observed in the spectra before and after CPL irradiation. This is

different from chirality induction to fluorene in which signal due to keto defect appeared in the IR spectra after irradiation.² The chemical structure changes of **S2** was further measured by ¹H NMR and SEC. To conduct these two measurements, a large scale experiment was carried out that 1 g of **S2** coated on NaCl were irradiated by CPL with 19 h. Even such a long time, still no chemical transform were indicated in ¹H NMR and SEC spectra (**Figure 4** and **5**).

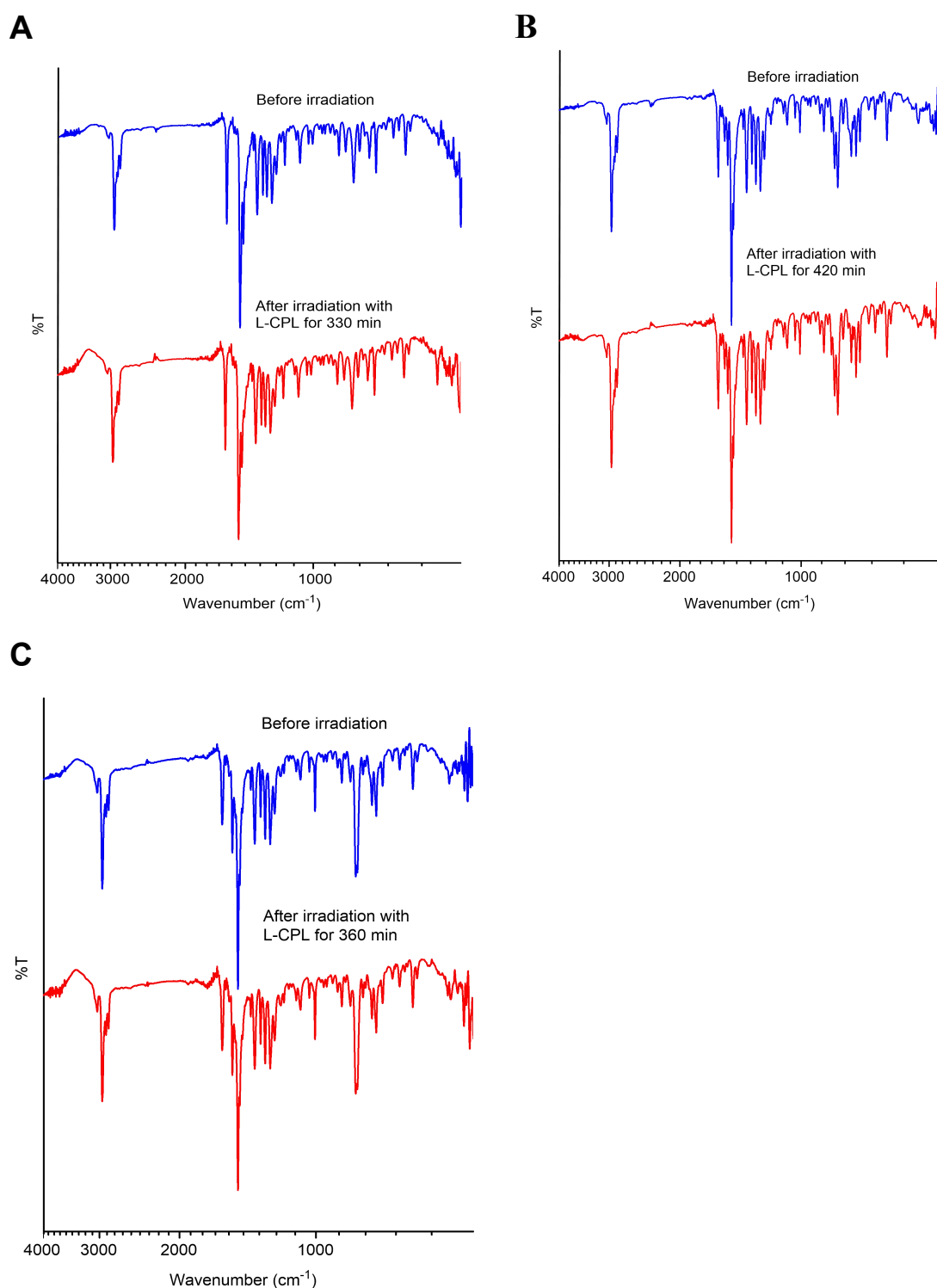


Figure 3. FT-IR spectra of S1, S2 and S3 (A, B, and C, respectively) films before and after irradiation with L-CPL. The CPL irradiation and IR measurements of the compounds were based on the films coated on NaCl plate.

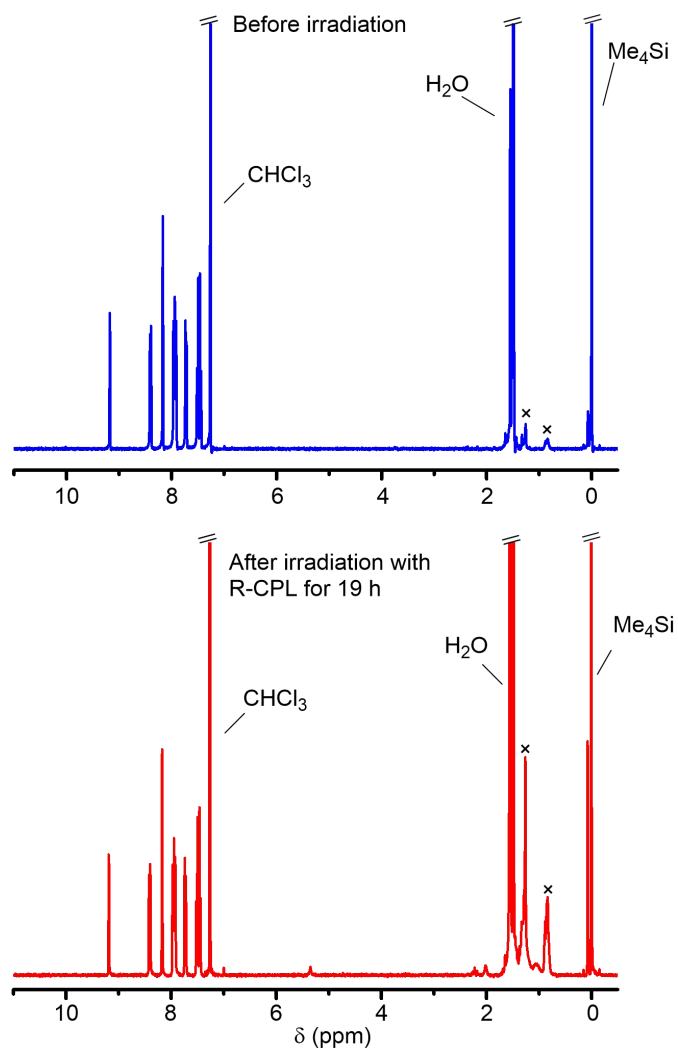


Figure 4. ^1H NMR spectra (400 MHz, CDCl_3) of S2 films before and after irradiation for 19 h with R-CPL. S2 was irradiated in a large amount that 1 mg sample was coated on a NaCl plate. The sample after irradiation was recovered by washing the NaCl plate with CHCl_3 , and recovered by removing the solvent.

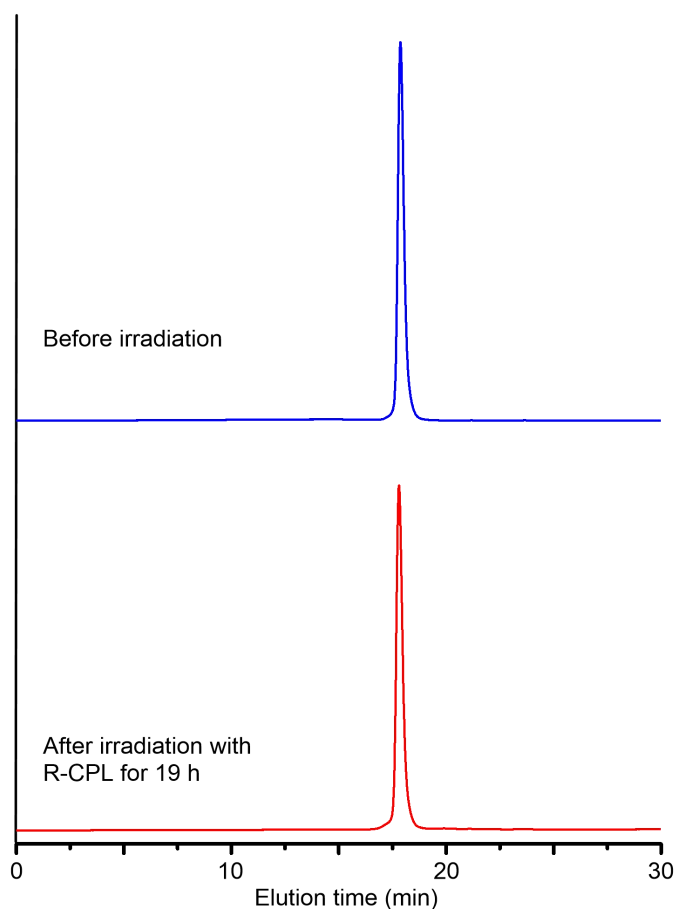


Figure 5. SEC curves of **S2** sample (the same sample used for ^1H NMR) before and after irradiation for 19 h with R-CPL.

Chirality of **S2** film can be conducted in a reversible way by switching the chirality of CPL light as shown in **Figure 6**. Firstly, 150 min irradiation of L-CPL produced a positive CD signal located at 368 nm with g_{CD} about 7.3×10^{-4} . This signal was erased by irradiation of R-CPL in 90 min. Continued to irradiate the sample by R-CPL, a clear negative signal arose, which is almost symmetrical to the signal produced by L-CPL. This peak also completely disappeared when a L-CPL irradiation was again applied to the film. So far, one circle of the chirality induction finished, and a second circle also can start by further irradiation of L-CPL. These results mean that Chirality switching is thus possible for the star molecules.

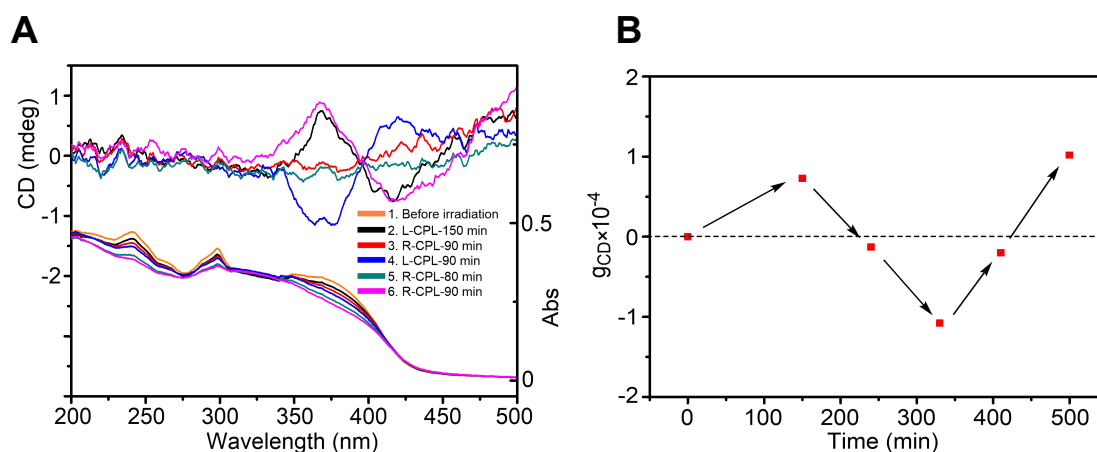


Figure 6. CD/UV spectra (A), and g_{CD} -vs.-time plot (B) for **S2** film irradiated with L-CPL and R-CPL alternately. The film was prepared from solution at 1.0×10^{-3} M. g_{CD} calculation were based on the wavelength of 368 nm.

3.3 Identification of Chiral Structure, Chirality Induction Mechanism, and Chirality Amplification

Molecular geometry optimization and theoretical CD calculations were performed to reveal the chiral structure induced by CPL. Because the three molecules have trigonal symmetry, chirality of one of the three arms stretching from the central benzene core will well explain chiroptical properties of the entire molecules. Hence geometry optimization of one-arm models was conducted by DFT and the optimized structures were displayed in **Figure 7 A-C**. The 2,5-diphenyl-1,3,4-oxadiazole moiety of the three molecules adapt a almost coplanar structure, which indicates that this moiety does not likely to contribute to observed CD spectra. In **S1** structure, the only chiral moiety is the N-phenylcarbazole which has a negative dihedral angle of -48 deg. Similar to **S1**, the N-phenylcarbazole moiety in **S2** also has a negative dihedral angle (-49 deg). Besides, a negative dihedral angle (-36 deg) for the biphenyl moiety can also be observed. **S3** has a negative dihedral angle (-49 deg) for the N-phenylcarbazole moiety and positive dihedral angles (+36 deg and +36 deg) for the terphenyl moiety having right-handed helical conformation. Thus, the three molecules have a negative twist around the C-N bond in common.

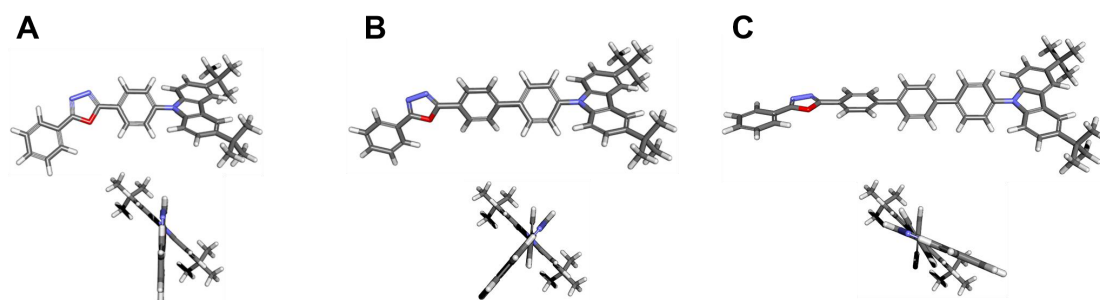


Figure 7. Optimized conformations of one arm structure of **S1**, **S2**, and **S3** (A, B, and C, respectively).

Figure 8 shows the theoretical CD spectra for the optimized one-arm models along with the corresponding experimental spectra. The theoretical spectra exhibit a negative Cotton band centered at around 350 nm as the major signal which are very similar to those of the corresponding experimental spectra obtained on R-CPL irradiation, indicating that the geometries in **Figure 7A-C** may be the most plausible structures of the arms of the three molecules. **S1**, **S2**, and **S3** are thus proposed to take novel, three-blade propeller conformations with their three blades having the same handedness of twisted moieties (**Figure 8 A-C**). Further, the fact that the three molecules indicate **S1**, **S2**, and **S3** showed similar theoretical CD spectra regardless of chirality of constituent moieties other than that of the N-phenylcarbazole moiety clearly indicates that the observed chiroptical properties are mainly contributed by the N-phenylcarbazole moiety.

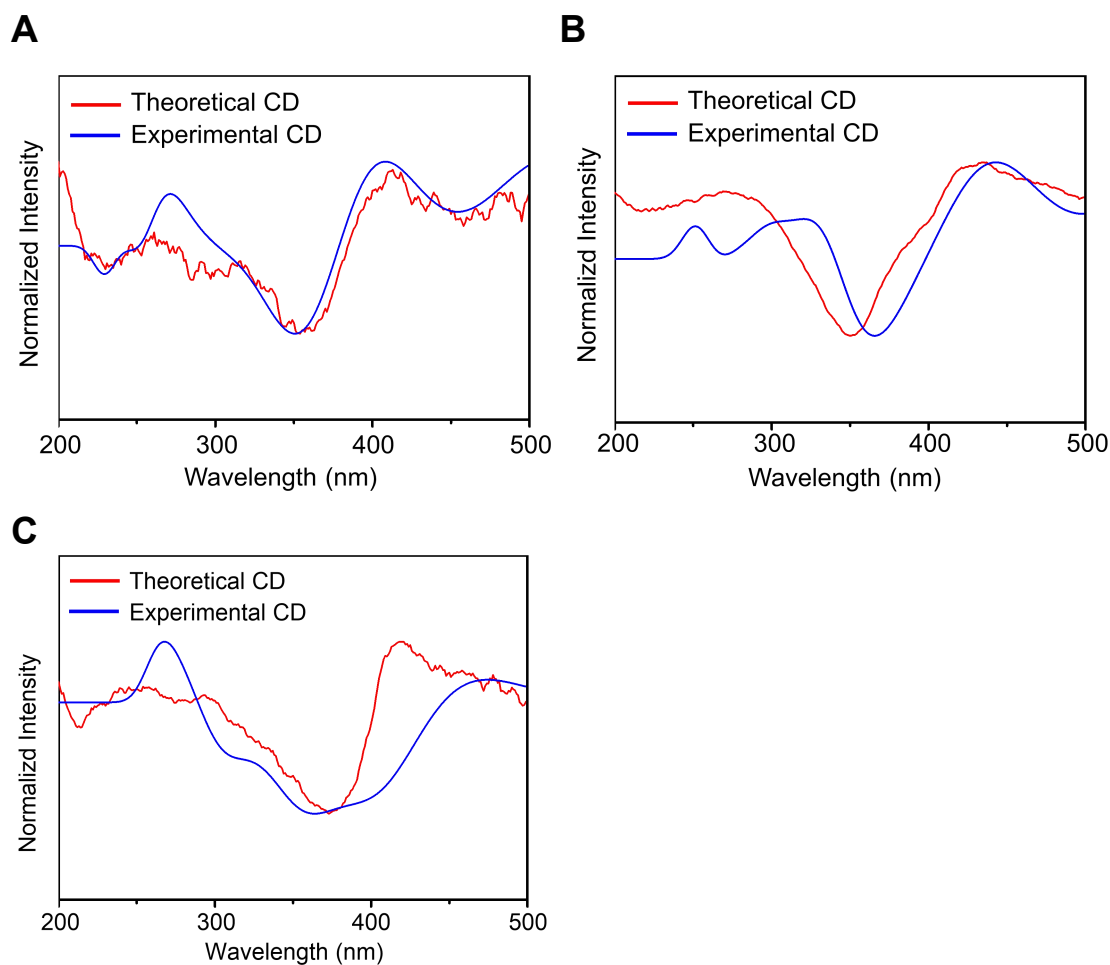


Figure 8. Theoretical CD spectra of the one-arm models and experimental CD spectra for **S1**, **S2**, and **S3** (A, B, and C, respectively). The experimental CD spectra correspond to those induced by R-CPL irradiation.

The formation of one handed twist of the N-phenylcarbazole moiety was ascribed to the enantiomer-selective photo excitation. Before CPL irradiation, the N-phenylcarbazole moiety in the three molecules were mixed by right and left handed twist in equal amounts. When the films were irradiated by CPL with particular direction, only one enantiomer of N-phenylcarbazole moiety was preferentially excited to the coplanar conformation, and deactivation of the excited species leads to both right- and left-handed twists. Hence, the twist which was not preferentially photo excited would become rich as the irradiation. Such a mechanism was also used to explain the helix induction to polyfluorene derivatives.^{2,3}

Much more information about the induction was disclosed by analyzing the detailed changes during the irradiation. **Figure 9A**, **10 A**, and **11A** show the changes

of CD and UV spectra on irradiation. The CD intensities of the three molecules increased with increasing irradiation time, and finally the irradiation was stopped when the CD intensity finished growth. Notably, UV absorbance decreased with an increase in irradiation time. The hypochromism can be ascribed to two structural features induced by light, i.e., formation of π -stacked aggregates⁴ and an increase in dihedral angles of the Ar-Ar moieties in the three molecules.⁵ The formation of aggregates was supported by molecular dynamics (MD) simulations showed that five **S2** molecules swiftly formed a densely π -stacked aggregate in **Figure 12**. Aggregation was experimentally evidenced for THF/H₂O solutions of the three molecules; addition of H₂O (poor solvent) to a THF (good solvent) solution can induce aggregation. Hypochromism was observed on an addition of water into **S2** solution as shown in **Figure 13**.

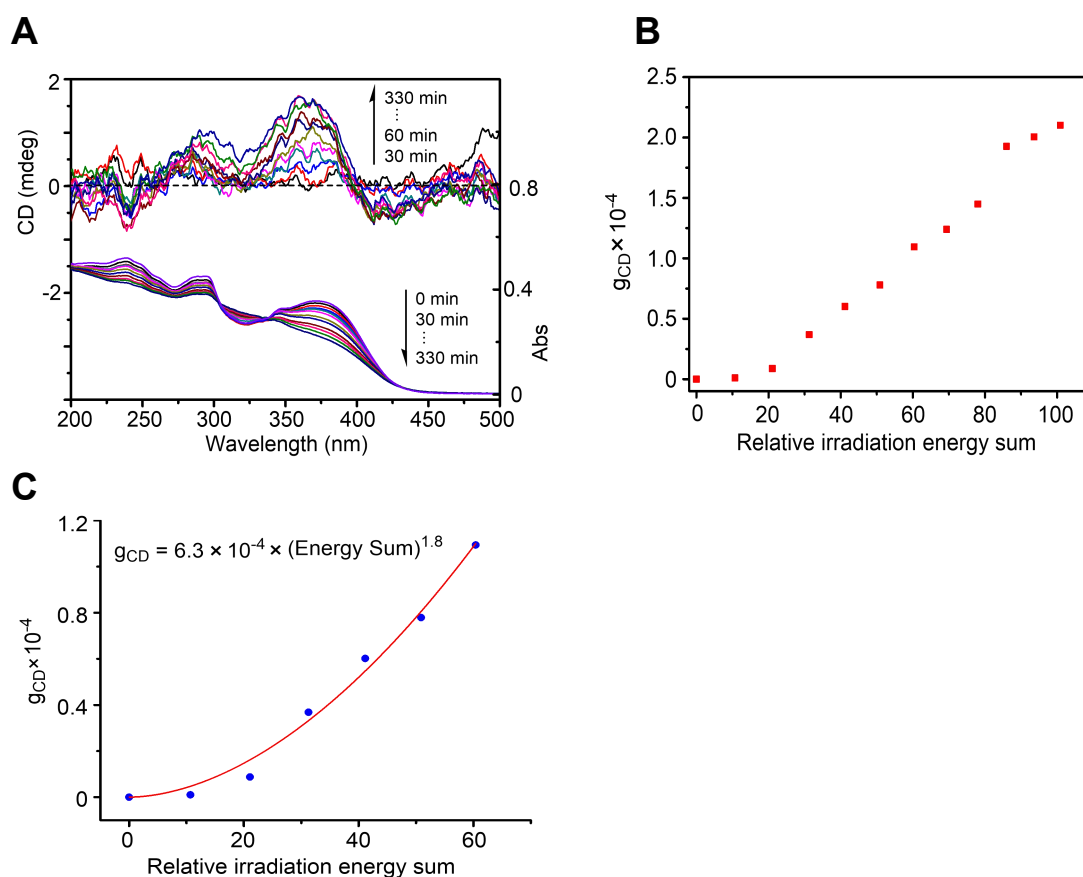


Figure 9. (A) changes in CD/UV spectra observed on L-CPL irradiation, (B) g_{CD} -relative irradiation energy sum plots for chirality induction on L-CPL irradiation, and (C) curve-fitting leading to a non-linear function approximation of the g_{CD} plot for **S1**. The films were prepared from solutions at 5.0×10^{-3} M.

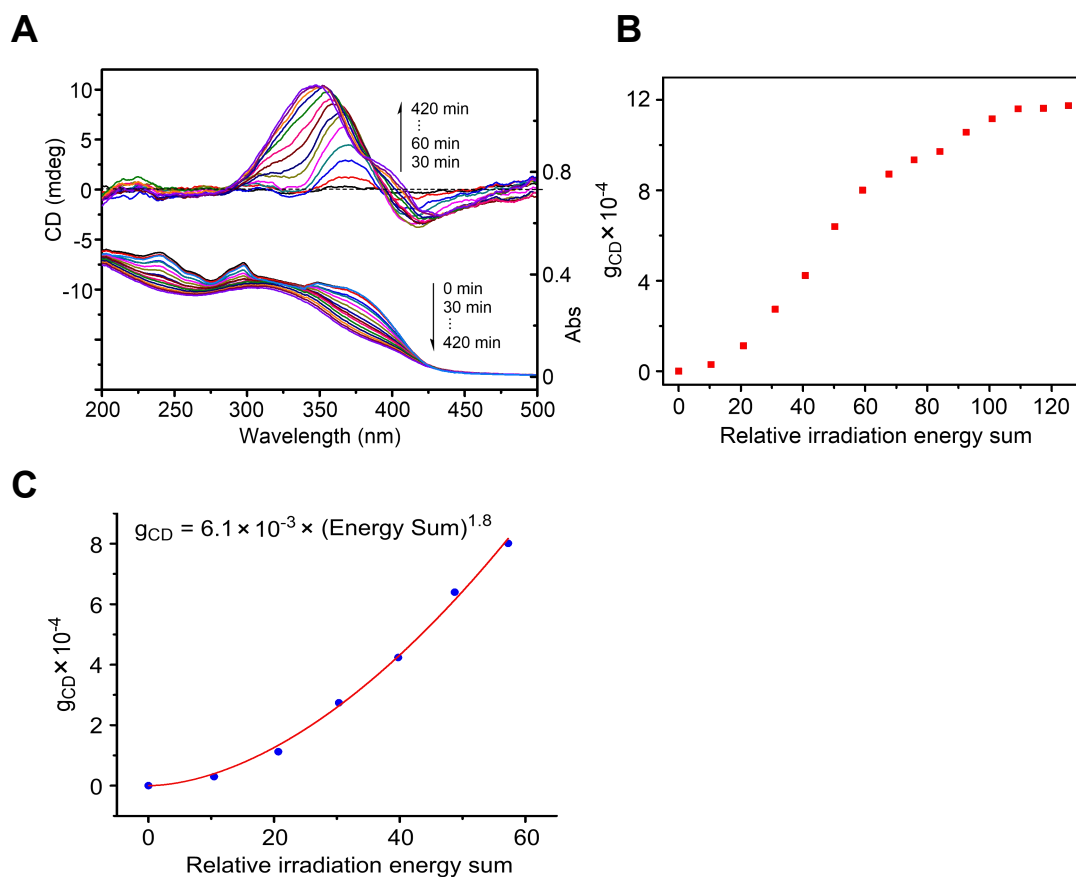


Figure 10. (A) changes in CD/UV spectra observed on L-CPL irradiation, (B) g_{CD} -relative irradiation energy sum plots for chirality induction on L-CPL irradiation, and (C) curve-fitting leading to a non-linear function approximation of the g_{CD} plot for **S2**. The films were prepared from solutions at 5.0×10^{-3} M.

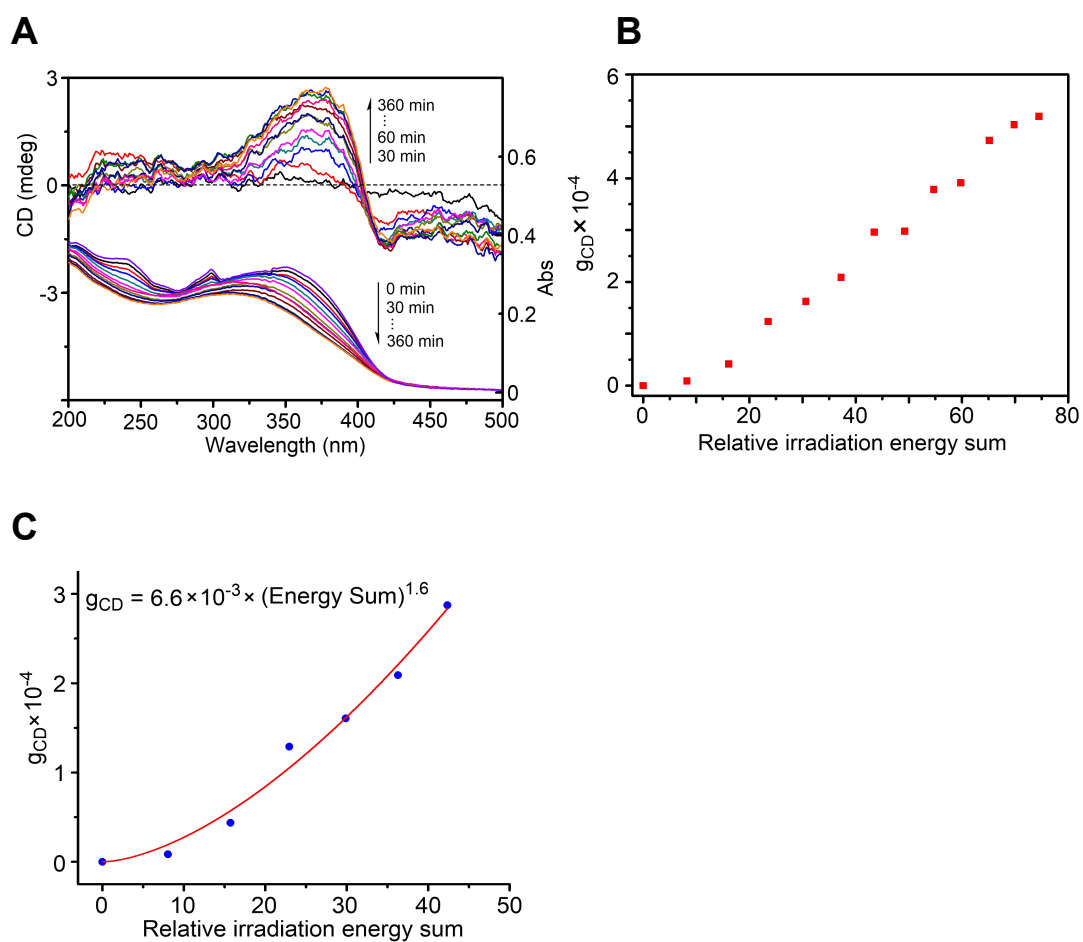


Figure 11. (A) changes in CD/UV spectra observed on L-CPL irradiation, (B) g_{CD} -relative irradiation energy sum plots for chirality induction on L-CPL irradiation, and (C) curve-fitting leading to a non-linear function approximation of the g_{CD} plot for **S3**. The films were prepared from solutions at 2.5×10^{-3} M.

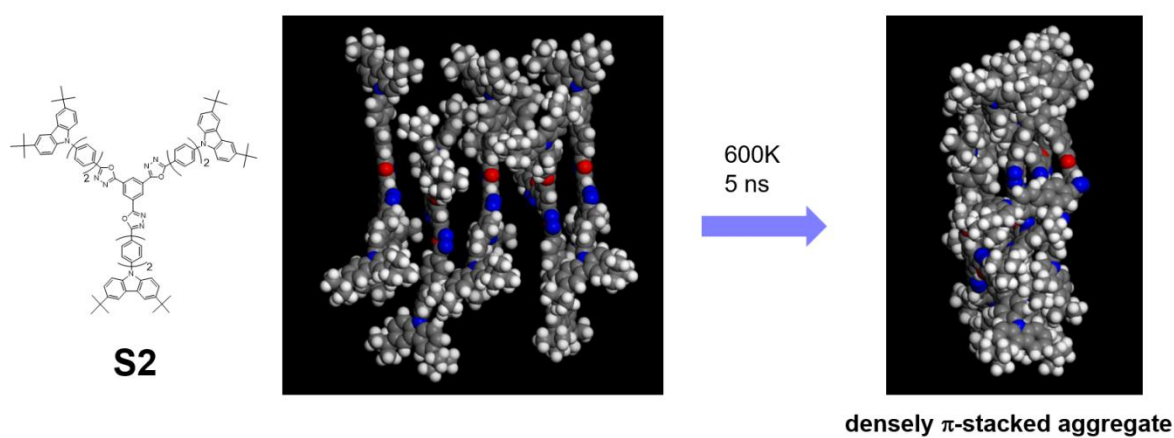


Figure 12. MD stimulation of **S2** molecules from dispersion to aggregation at 600 K.

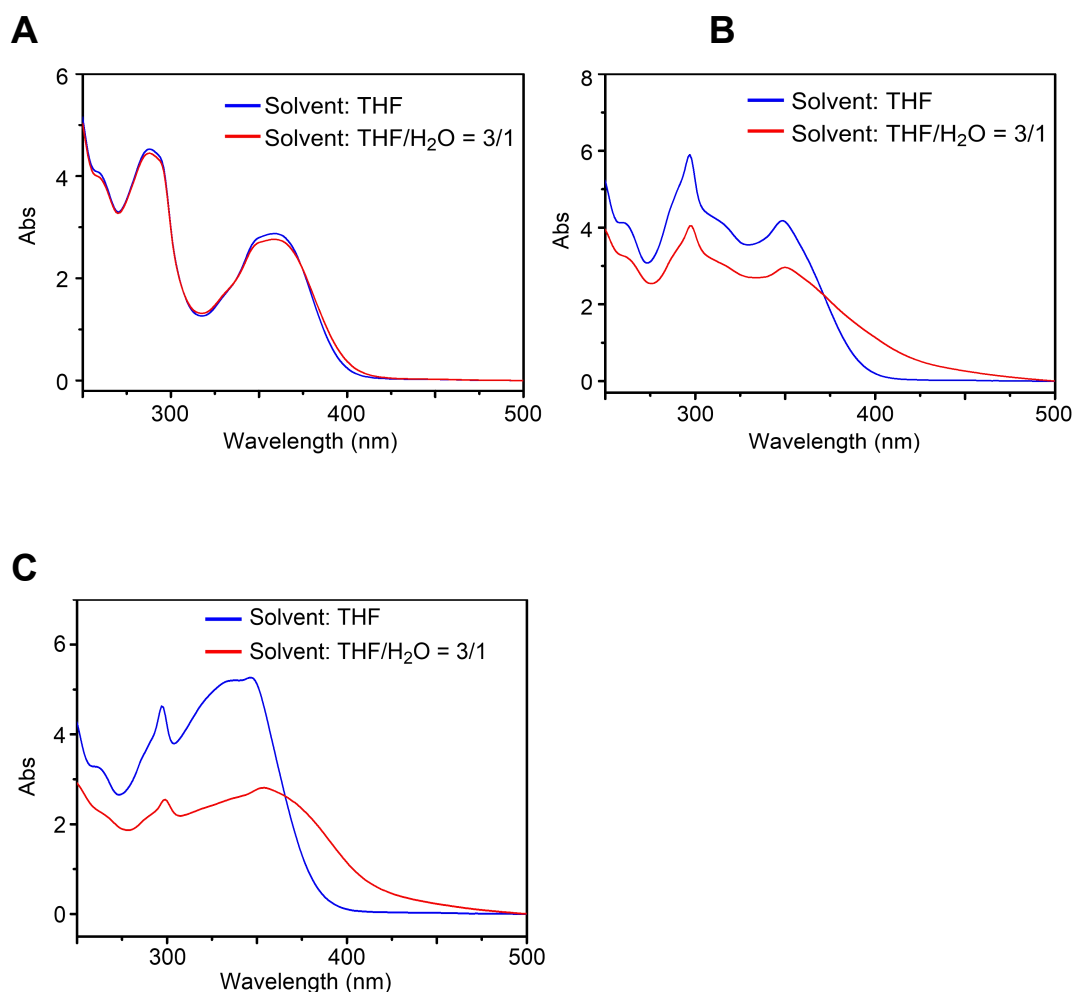


Figure 13. UV spectra of **S1**, **S2**, and **S3** (A, B, and C, respectively) in pure THF and THF/H₂O mixed solvent. The concentration of the three molecules in THF and mixed solvent were identical with the value of 3.8×10^{-6} M.

The extent of chirality induction was evaluated in terms of Kuhn's anisotropy factor (g_{CD}). **Figure 9B**, **10 B**, and **11B** show the plots of g_{CD} against relative irradiation energy sum. g_{CD} increased with the irradiation time and finally leveled up with the values of 2.1×10^{-4} for **S1**, 1.2×10^{-3} for **S2** and 6.1×10^{-4} for **S3**. Among these results, **S2** reached the highest g_{CD} values. The g_{CD} values of these three molecules are comparable to those of single enantiomer of axially chiral, small molecules, suggesting that the three molecules have almost single-handed twisted conformation.⁶ In addition, irradiation of CPL alone only can lead to g_{CD} around $10^{-6} \sim 10^{-8}$ order,^{6a-c} thus the present result strongly indicates that chirality amplification was involved in

the induction process.

It is noteworthy that the data points in the g_{CD} -relative irradiation energy sum plots in the early stages of irradiation can be fitted by a power function (**Figure 9C, 10C, and 11C**). Without chirality amplification, the g_{CD} -vs.-relative irradiation energy sum plots would have a curve shape similar to a conversion-vs.-reaction time plot for 1-st order chemical reactions which has an increasing form of exponential decay, $g_{CD} = A_0(1 - e^{-(\text{relative irradiation energy sum})})$. The fact that the early stage data points in **Figure 9C, 10C, and 11C** are well approximated with power functions, $g_{CD} = a(\text{relative irradiation energy sum})^b$, for the early stages of chirality induction strongly supports that chirality is amplified.

The mechanism of chirality induction to the three molecules is proposed to be based on enantiomer-selective photo excitation of the axially chiral moieties in the molecular structures. Compounds having aromatic-aromatic (Ar-Ar) diad structure represented by biphenyl with chiral, twisted conformation are known to transform into achiral, coplanar structure on photo excitation (TCT), and enantiomer-selective excitation of right- or left- handed twist leads to enrichment of the unexcited twist. In the structures of the three molecules, twisted conformations are found for phenyl-phenyl and N-phenylcarbazole moieties in the ground state. Although coplanar conformation of N-phenylcarbazole in excited states has not been explicitly identified so far,⁷ such a conformation is proposed to be involved as a transient species in the chirality induction. On photo excitation with R-CPL, right-handed twisted N-phenylcarbazole moiety is preferentially excited into coplanar conformation which produces both right- and left-handed twists on deactivation to the ground state where chirality amplification is proposed to occur. Intermolecular interactions between coplanarized N-phenylcarbazole moiety in excited states and single-handed twisted, ground-state N-phenylcarbazole moiety in the vicinity which has already been made single-handed twisted through earlier-stage CPL-excitation and deactivation may lead to biased deactivation to the hand which is the same as the ground-state N-phenylcarbazole moiety through synergy effects (“deactivation

chirality amplification”).

It is intriguing that the biphenyl moiety in **S2** and the terphenyl moiety in **S3** led to left- and right-handed chirality (helicity) on irradiation with L-CPL; the two chromophors have reversed sensitivity toward the same hand of CPL chirality in this case.

3.4 Effect of Aggregates and Inter-molecular Ordering on Chirality Induction.

During the chirality induction, we found that the films made by solutions with different concentrations gave different behavior under same CPL irradiation condition. **Figure 14-16** are the results of films made from solutions at concentration of 1.0×10^{-3} M for all the three molecules. It is intriguing that **S1** film can't be induced into optically active even the irradiation time were extended to 420 min. For **S2** and **S3** films made by 1.0×10^{-3} M solutions, the chirality induction were successful. But the g_{CD} values were lower than that of the above mentioned films made from solutions at 5.0×10^{-3} M and 2.5×10^{-3} M. This trend can be clearly observed from the g_{CD} plots in **Figure 14C**, **15C**, and **16C**. Absorbing same amount of energy, films made by higher concentration solutions had higher g_{CD} values. Beside, the films made by high concentration solutions also led to a greater maximum g_{CD} values when the g_{CD} plot leveled up.

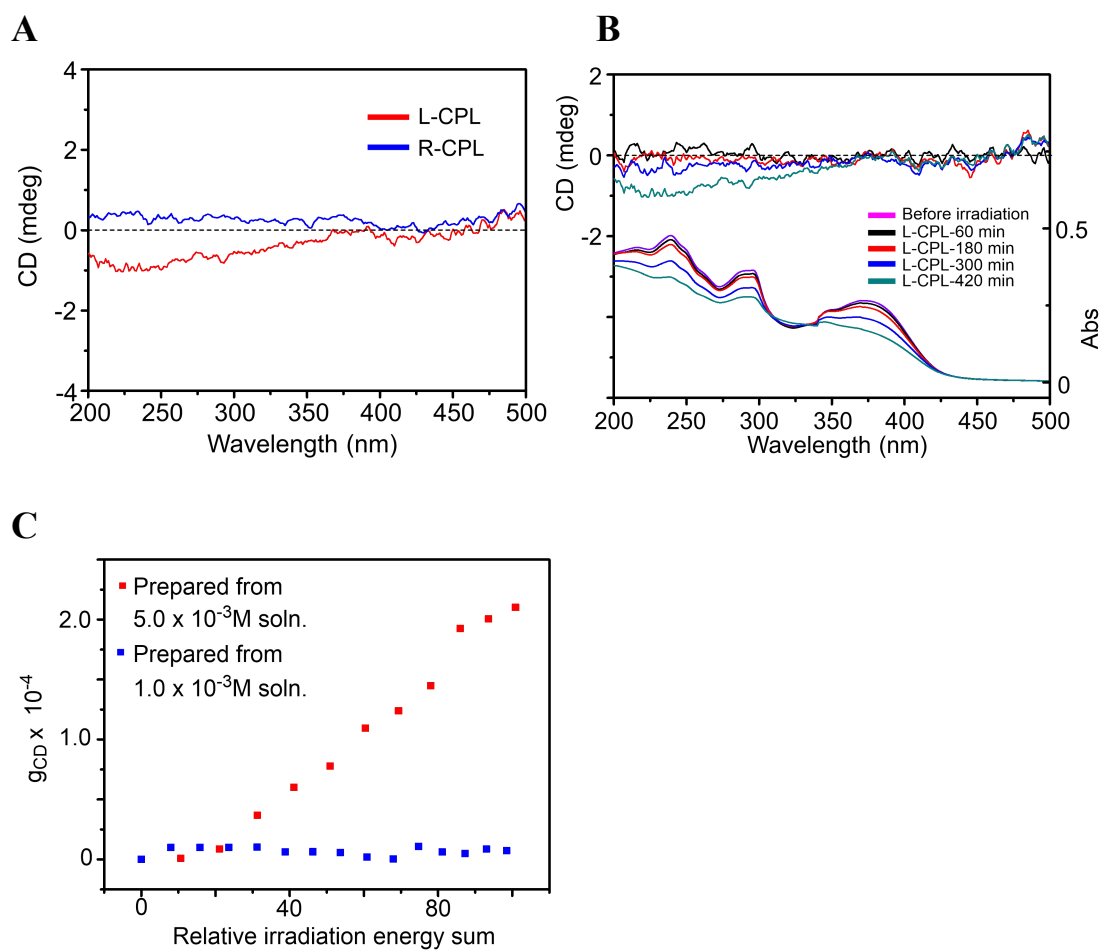


Figure 14. CD spectra after L and R-CPL irradiation (A), CD/UV spectra upon L-CPL irradiation (B) for **S1** films prepared from solution at $1.0 \times 10^{-3} M$, and g_{CD} -vs.-relative irradiation energy sum plots (C) for **S1** prepared from solution at $5.0 \times 10^{-3} M$ and $1.0 \times 10^{-3} M$.

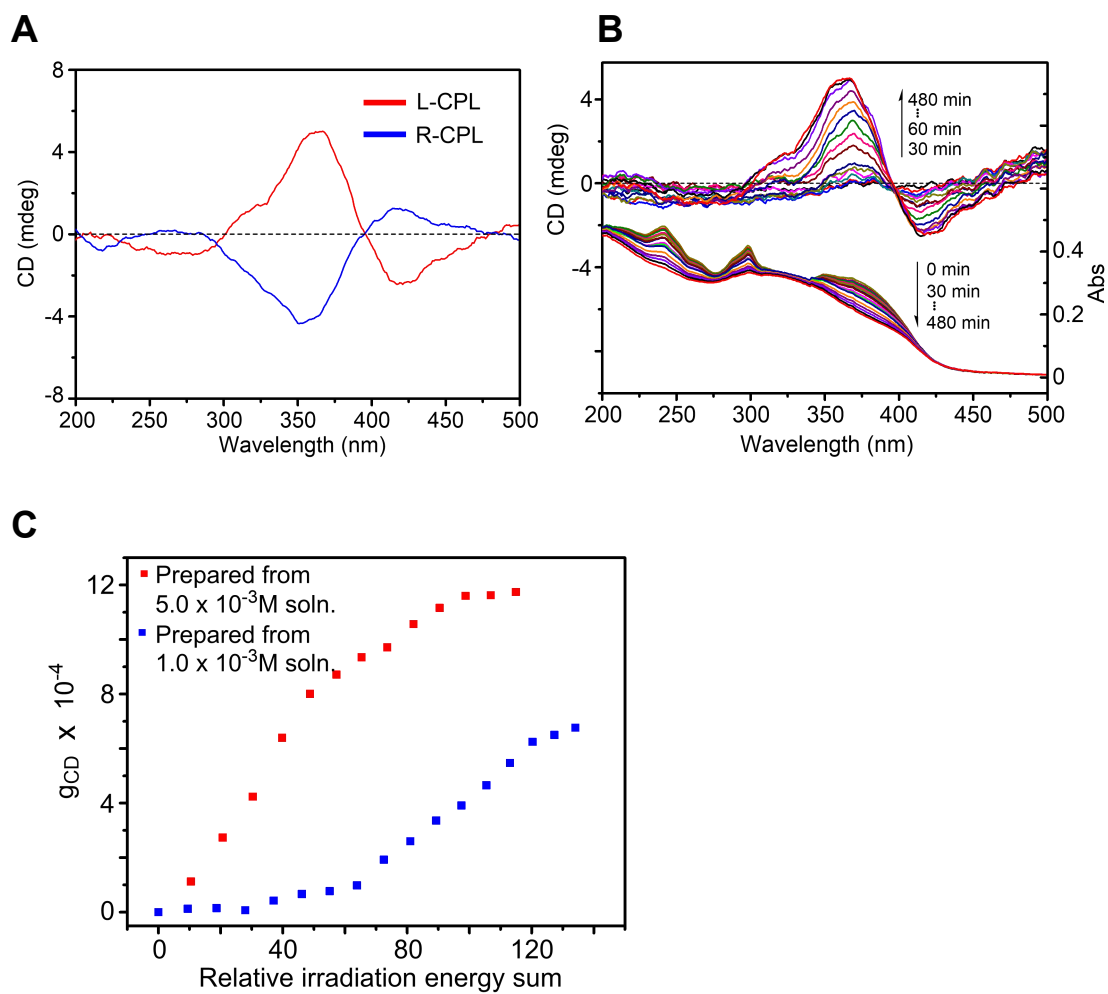


Figure 15. CD spectra induced by L- and R-CPL irradiation (A), changes in CD/UV spectra observed on L-CPL irradiation (B), and g_{CD} -vs.-relative irradiation energy sum plots prepared from solution at $1.0 \times 10^{-3} M$, and g_{CD} -vs.-relative irradiation energy sum plots (C) for **S2** prepared from solution at $5.0 \times 10^{-3} M$ and $1.0 \times 10^{-3} M$.

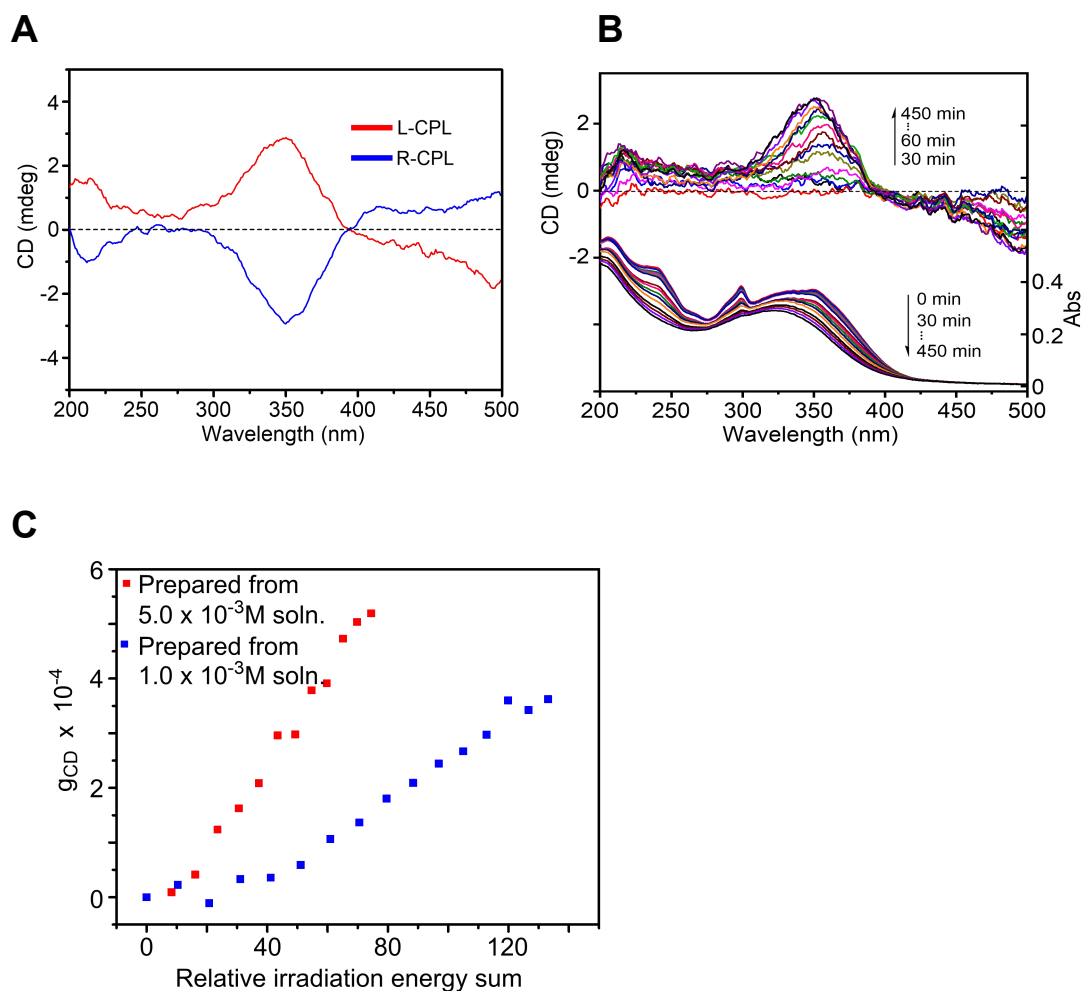


Figure 16. CD spectra induced by L- and R-CPL irradiation (A), changes in CD/UV spectra observed on L-CPL irradiation (B), prepared from solution at $1.0 \times 10^{-3} M$, and g_{CD} -vs.-relative irradiation energy sum plots (C) for S3 prepared from solution at $2.5 \times 10^{-3} M$ and $1.0 \times 10^{-3} M$.

From the above mentioned results, it can be proposed that a higher concentration may facilitate intermolecular interactions leading to a film morphology suitable for chirality amplification. This idea was supported by dynamic light scattering of S2 solutions. The mean diameter of S2 in $1.0 \times 10^{-3} M$ solution was 4.6 nm whereas that values for $5.0 \times 10^{-3} M$ solution was 13.5 nm, which indicates that the formation of aggregates in solution is facilitated at a higher concentration (Figure 17).

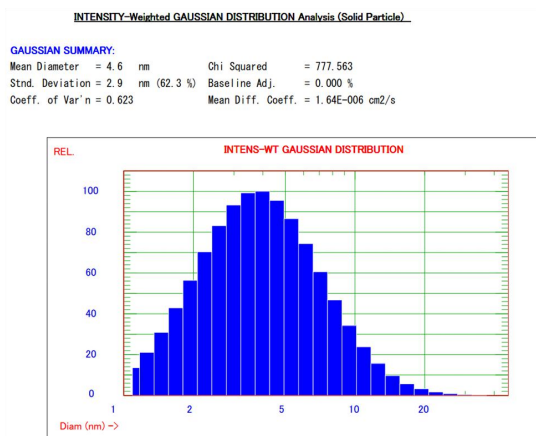
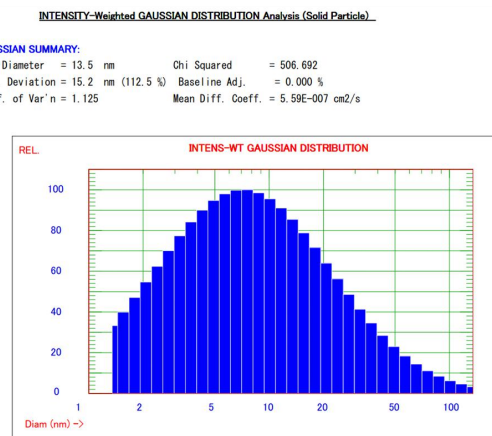

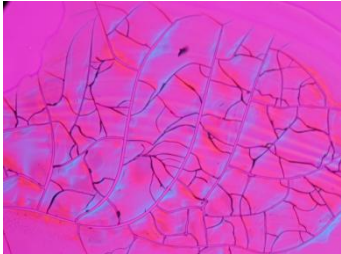
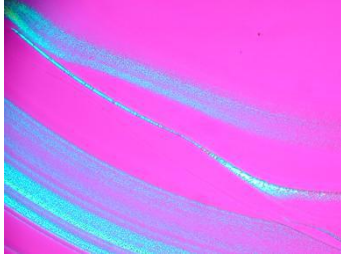
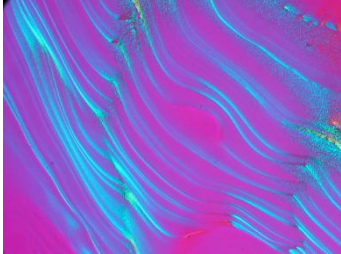

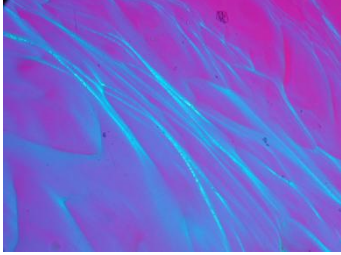
A**B**

Figure 17. Particle size distributions of **S2** in chloroform with concentration of 1.0×10^{-3} M (A) and 5.0×10^{-3} M (B) obtained by dynamic light scattering.

Table 1 exhibits the polarized optical microscope (POM) results of the molecules, which supports that films made at higher concentrations have some ordering of molecules. Though the crystal structures in **S1** films was not so obvious, **S2** and **S3** films display distinct crystal structure. What's more, the films made by high concentration solutions tend to have much dense crystal structure than that in the films made by low concentration solutions. The significance of such ordering to chirality induction was further identified by the chirality induction of the annealed films in **Figure 18** and **19**. Films of **S2** and **S3** showing textures based on molecular ordering in POM observations were heated at 320°C or 340°C to lead to isotropic films showing no textures. The heating only changed the morphology of the films but the molecular structures was not destroyed indicating by the IR spectra. Then the isotropic films were irradiated with CPL. however, chirality was failed to be induced.

Table 1. Morphologies of films.

Molecule	Polarized optical microscopic texture for the films cast from solutions at lower concentrations	Polarized optical microscopic texture for the films cast from solutions at higher concentrations
S1	 $1.0 \times 10^{-3} \text{ M}$	 $5.0 \times 10^{-3} \text{ M}$
S2	 $1.0 \times 10^{-3} \text{ M}$	 $5.0 \times 10^{-3} \text{ M}$
S3	 $1.0 \times 10^{-3} \text{ M}$	 $2.5 \times 10^{-3} \text{ M}$

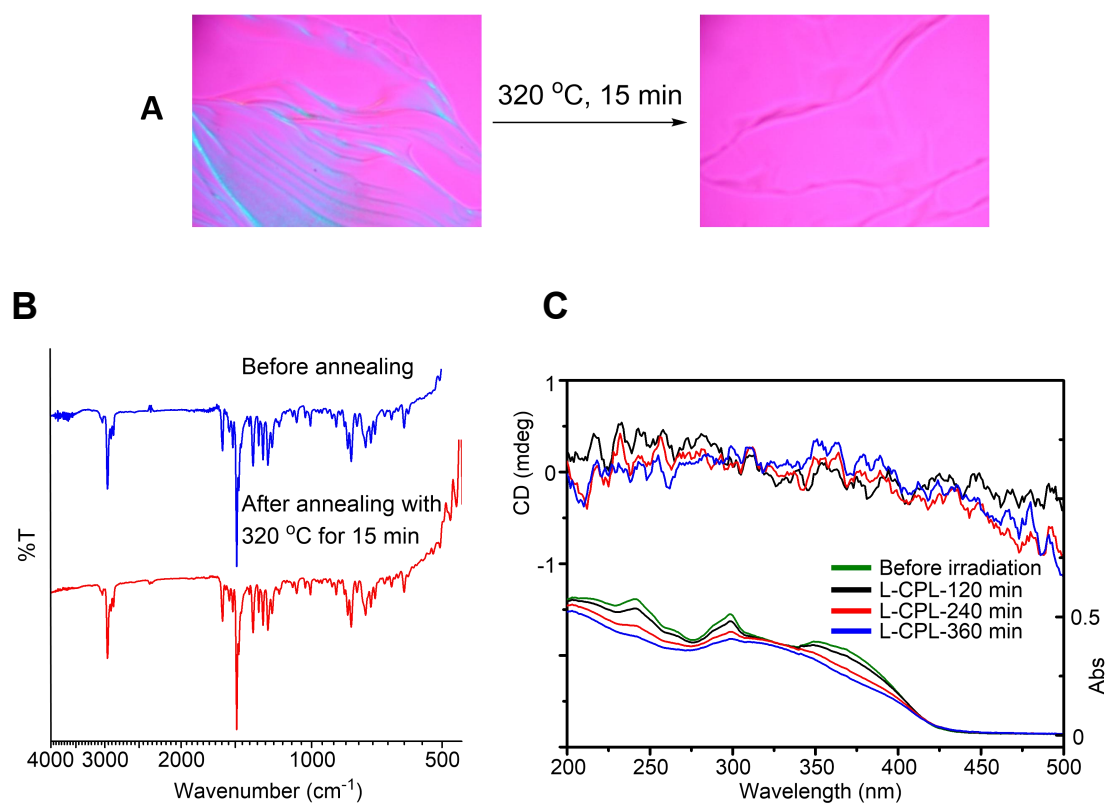


Figure 18. Polarized optical micrographs (A) and FT-IR spectra (B) of **S2** films before and after annealing (320 °C, 15 min), and CD/UV spectra of the isotropic **S2** film on irradiation of L-CPL (C). The film was prepared from solution at 1.0×10^{-3} M on a quartz plate.

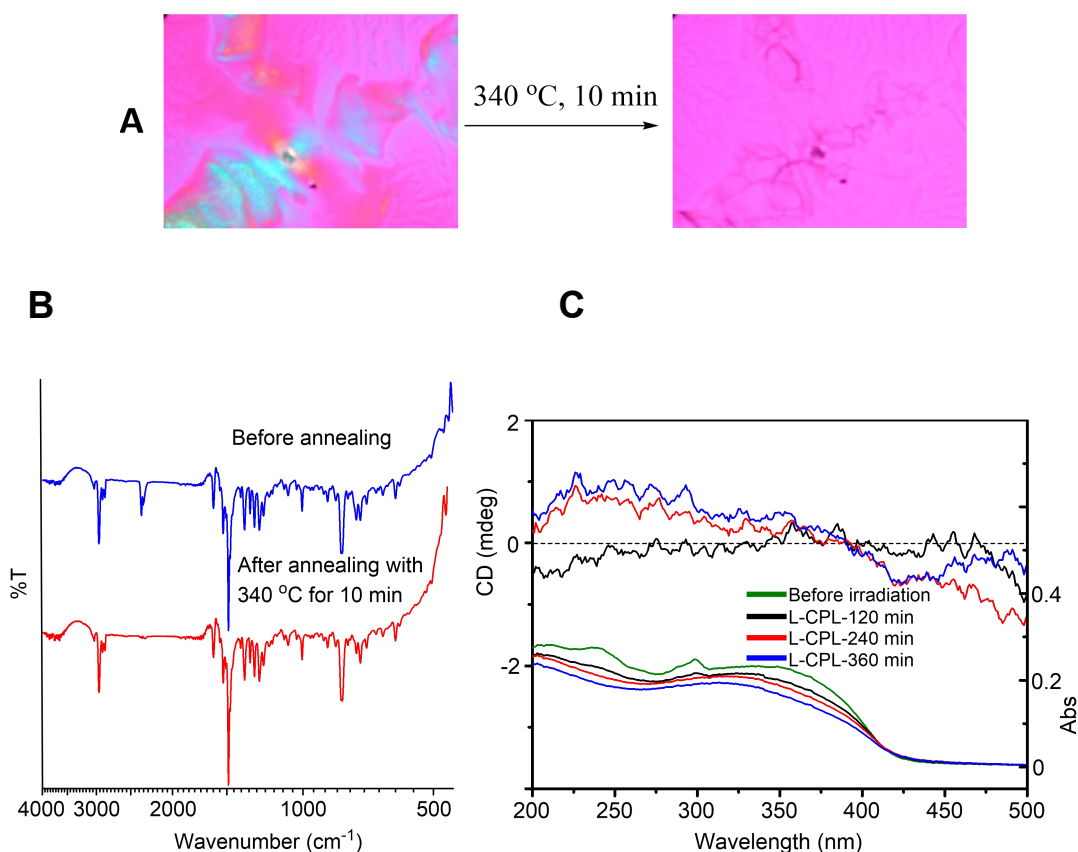


Figure 19. Polarized optical micrographs (A) and FT-IR spectra (B) of **S3** films before and after annealing (340 °C, 10 min), and CD/UV spectra of the isotropic **S3** film on irradiation of L-CPL (C). The film was prepared from solution at 1.0×10^{-3} M on a quartz plate.

3.4 Chirality Induction to the Oligomers In the Presence of Fluorene

Using fluorene as an aid molecule in T3 film can realize its chirality induction by improving the intermolecular interactions.^{3b} To study whether this method is applicable to these three molecules, CPL irradiation on their films in the presence of aid molecule were also conducted (**Figure 20**). With the participation of fluorene, chirality induction to **S1** film made by 1.0×10^{-3} M solution became possible, and relative high g_{CD} was achieved with the value about 5.0×10^{-4} . For **S2** and **S3**, strong CD signals can be observed in the spectra (**Figure 20 C and E**), and the g_{CD} values of films mixed with fluorene enhanced much compared with their pure films. In addition, the maximum values of g_{CD} even greater than that of the films made by high concentration solution. These results further proved that using aid molecule can

improve the intermolecular interactions of the film, and it is an effective method to improve chirality induction.

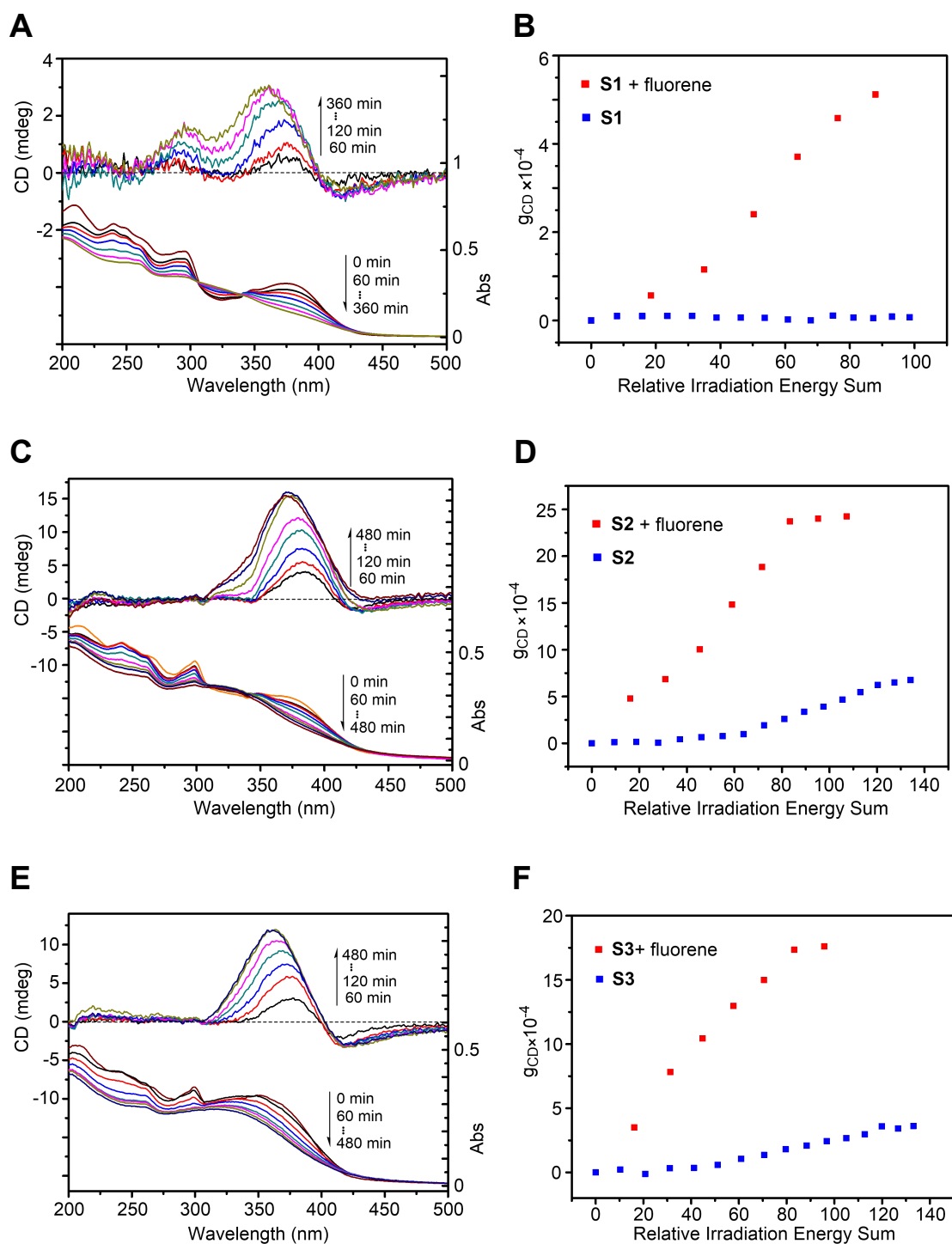


Figure 20. Changes in CD/UV spectra observed on L-CPL irradiation to films of S1, S2, and S3 mixed with fluorene (A, C, and E, respectively), and g_{CD} -relative irradiation energy sum plots for chirality induction of S1, S2, and S3 with fluorene and without fluorene (B, D, and F, respectively) on L-CPL irradiation. The films were prepared from solutions with a ratio of 1/3 to the oligomers (1.0×10^{-3} M) and fluorene (3.0×10^{-3} M).

3.5 Stability of induced chirality.

The stability of CPL induced chiral structures was examined by heating in the dark and irradiating with NPL. The optically active **S2** films were prepared by L-CPL irradiation. As for the thermal stability, the CD signal only changed little on heating at 150 °C for 72 h (**Figure 21 A**). Further improved the temperature to 220 °C, the signal still can be maintained without big change in 60 min. The elimination of the CD signal occurred in 20 min until the temperature up to 320 °C. On the other hand, irradiation with NPL (1.03 W/cm²) resulted in a much faster decrease in CD intensity, and the CD signal almost completely disappeared in the range of 300-400 nm within 12 min. These results indicate that the induced chirality of the star-shaped molecule films is rather stable against heat while is readily racemized on strong light irradiation.

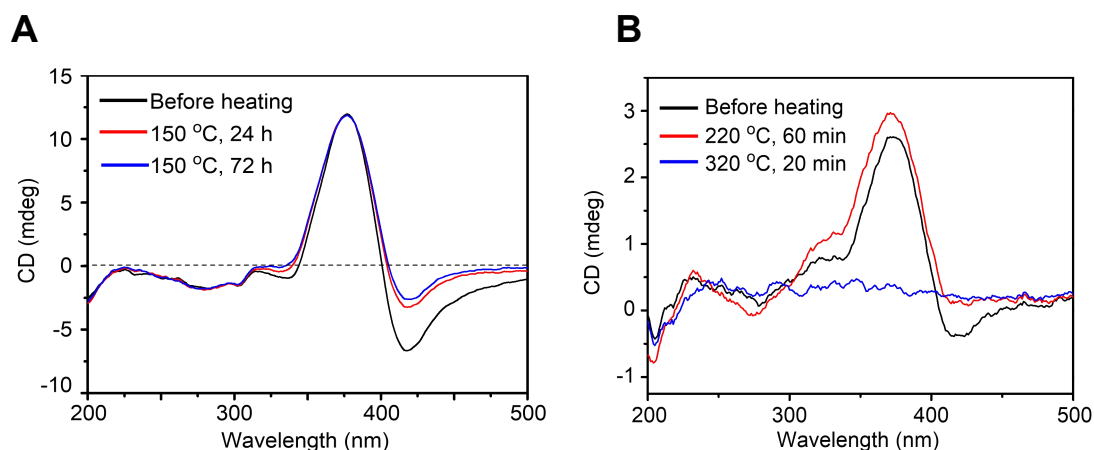


Figure 21. CD spectra of optically active **S2** films on heating with 150 °C (**A**) and 220/320 °C (**B**). The films were prepared from solution at 5.0×10^{-3} M on quartz plates, and the initial CD signal was induced by L-CPL.

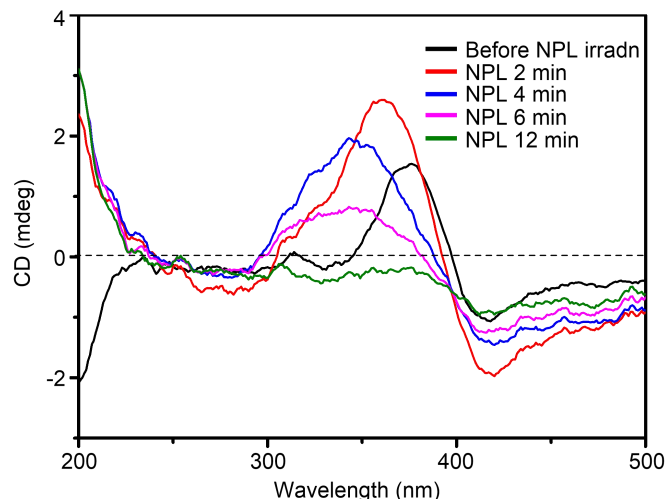


Figure 22. CD spectra of optically active **S2** films on irradiation with non-polarized light. The films were prepared from solution at 5.0×10^{-3} M on quartz plates, and the initial CD signal was induced by L-CPL.

3.6 Circularly Polarized Luminescence of Optically Active Films.

Because these three oligomers are good blue emitters, their anisotropic emission after chirality induction would be an intriguing property from a view of application for OLED. Hence, their circularly polarized luminescence (CPL emission) were measured. As shown in **Figure 23**, CPL emission of **S1** film was very weak, and the shapes of the signals were difficult to be read due to the disturbance of the noise. While rather strong signal can be observed for **S2** and **S3**, and the films induced by L- and R-CPL exhibited almost mirror CPL emission spectra.

The extent of anisotropy in circularly polarized luminescence was evaluated in terms of g_{lum} according to the following equation:

$$g_{lum} = 2(I_L - I_R)/(I_L + I_R)$$

where I_L and I_R are emission intensities of left-handed and right-handed CPL. The maximum g_{lum} values for **S2** and **S3** were -3.1×10^{-2} and -3.8×10^{-3} , respectively, while the g_{CD} values for **S2** and **S3** were 1.2×10^{-3} and 6.1×10^{-4} , respectively. The g_{lum} values were more than an order of magnitude higher than the corresponding g_{CD} values, suggesting that the two molecules have much higher anisotropy in excited

states than in the ground state. Chirality may be largely amplified for **S2** and **S3** on photo excitation through conformational transition of the molecules or changes in intermolecular aggregate structure. As for **S1**, photo excitation to **S1** may not remarkably amplify chirality. Thus, the benzene-1,4-diyl groups for **S2** and the biphenyl-4,4'-diyl groups for **S3** connecting the central benzene ring and the 2,5-diphenyl-1,3,4-oxadiazole moiety play important role in chirality amplification on photo excitation, leading to efficient CPL emission though they do not contribute to the CD spectra observed on chirality induction.

The excitation spectra of the films were measured, and the results are shown in **Figure 24**. The spectra of **S1** showed less remarkable differences before and after irradiation whereas the films of **S2** and **S3** changed a lot compared with their excitation spectra before irradiation. These observations support the changes in electronic structure of films of **S2** and **S3** on CPL irradiation, which may have a connection to the proposed morphological changes associated with the chirality amplification.

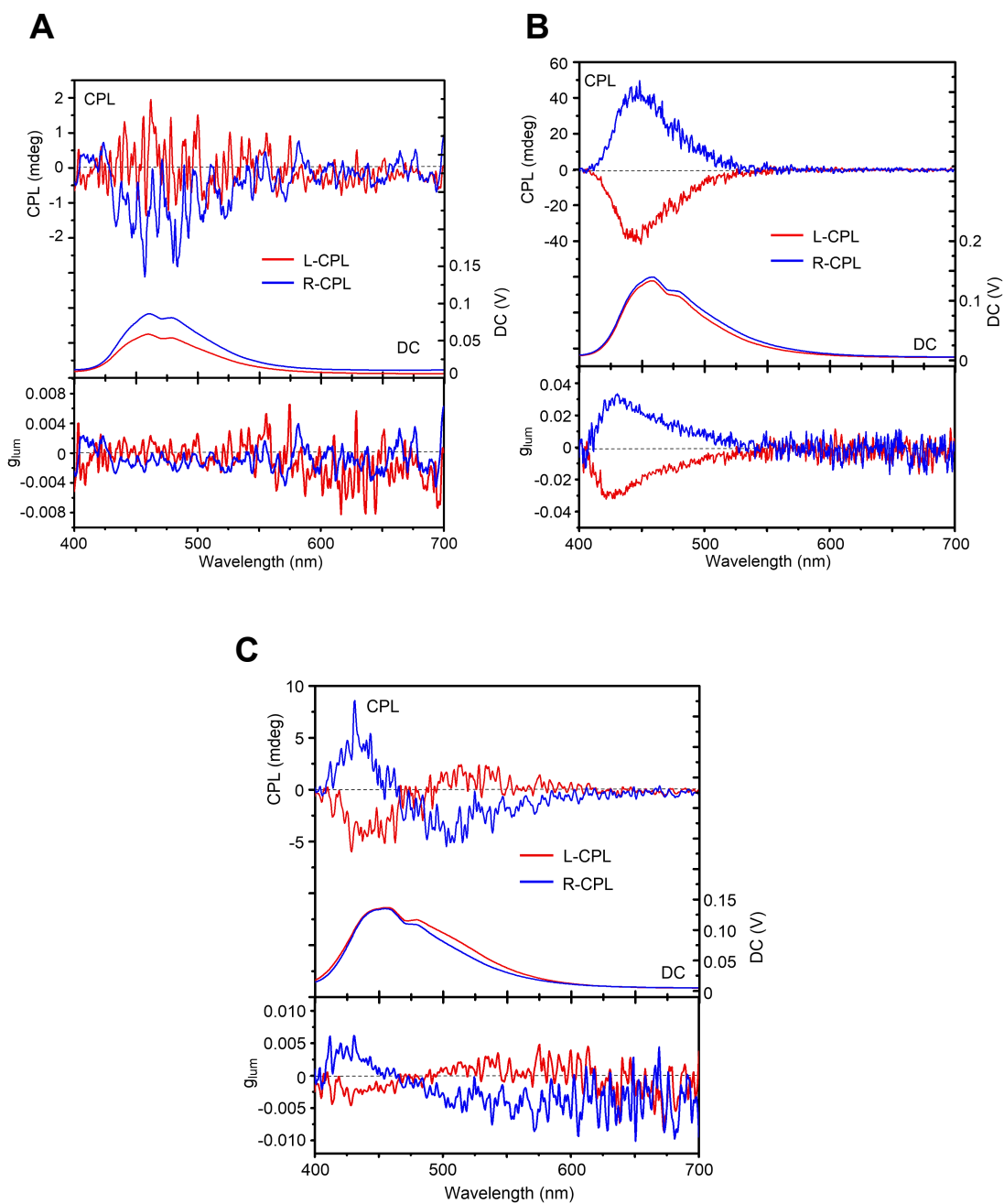


Figure 23. CPL, emission and g_{lum} spectra of **S1**, **S2**, and **S3** with induced chirality (A, B, and C, respectively) [λ_{ex} 350 nm]. The films were prepared from solutions at the following concentrations: 5.0×10^{-3} M for **S1** and **S2** and 2.5×10^{-3} M for **S3**).

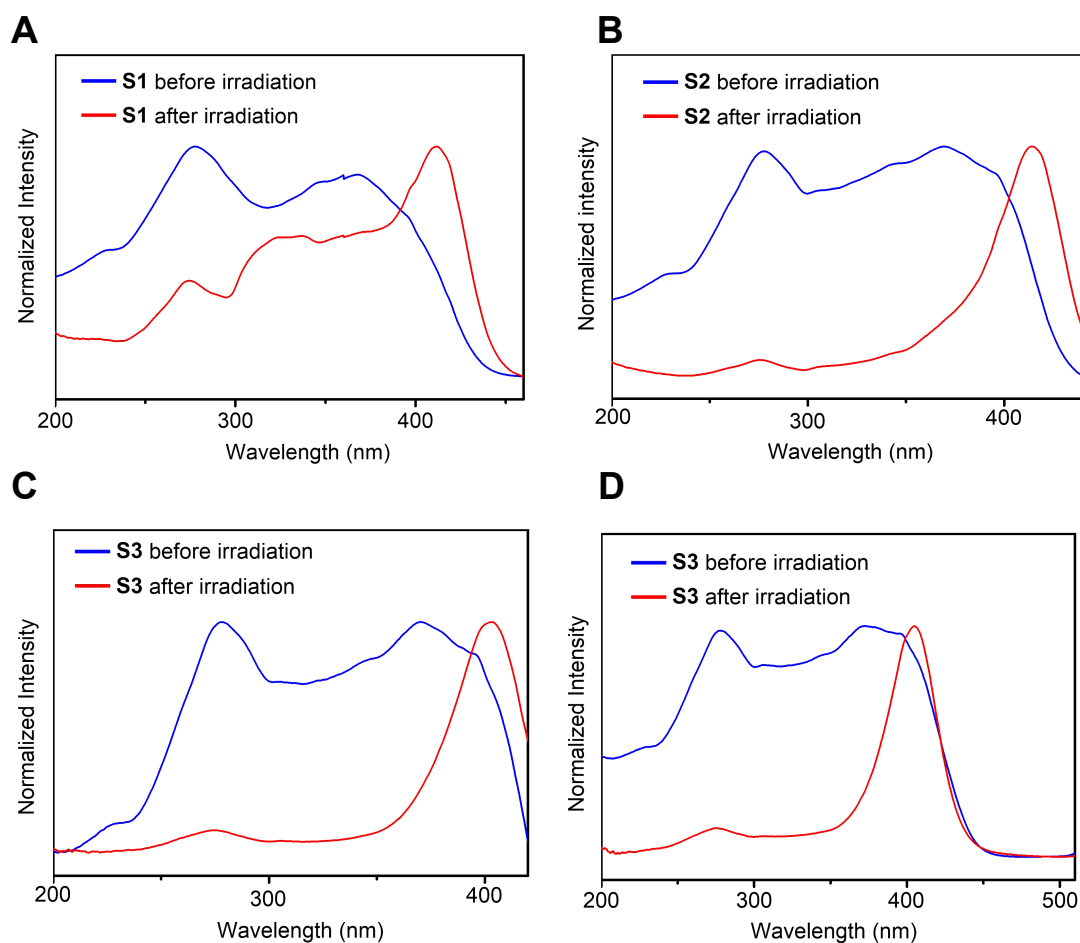


Figure 24. Excitation spectra of **S1** (A, $\lambda_{em} = 470$ nm), **S2** (B, $\lambda_{em} = 450$ nm), and **S3** (C, $\lambda_{em} = 430$ nm; D, $\lambda_{em} = 520$ nm) films before and after L-CPL irradiation. The films were prepared from solutions at 5.0×10^{-3} M for **S1** and **S2** and at 2.5×10^{-3} M for **S3**.

The CPL spectra of **S2** have monotonous shapes with signals located around 445 nm. As for the spectra of **S3**, in addition to the similar emission band to **S2**, a lower-energy emission bands with opposite signs also can be observed. At the same time, it can be found that the emission spectra of **S3** after irradiation appeared a shoulder peak centered at around 525 nm while the shoulder is not clear in the spectra of **S2**. This band may be assigned to the excimer emission and corresponds to the lower-energy CPL emission band. CPL emission of excimer was also reported in ref. 8 in which the emission of monomer and excimer also had opposite sign. The higher-energy CPL emission band of **S3** seems to correspond to the main, total

emission band centered at around 450 nm, which is common for the three molecules. Therefore, the CPL emission spectra of **S3** are thus proposed to be contributed by two excited states with different energies and opposite hands of chirality.

It may be noteworthy that the one-arm model of **S3** has two opposite twist senses coexisting in the same molecule, i.e., a negative twist around the C-N bond and positive twists for the terphenyl moiety. It is assumed that the higher-energy CPL emission band is mainly contributed by the N-phenylcarbazole moiety and the lower-energy CPL emission band mainly by the terphenyl moiety. The terphenyl moiety may induce π -stacked excimer formation between **S3** molecules while the carbazole moiety may be too bulky for excimer formation due the presence t-butyl groups.

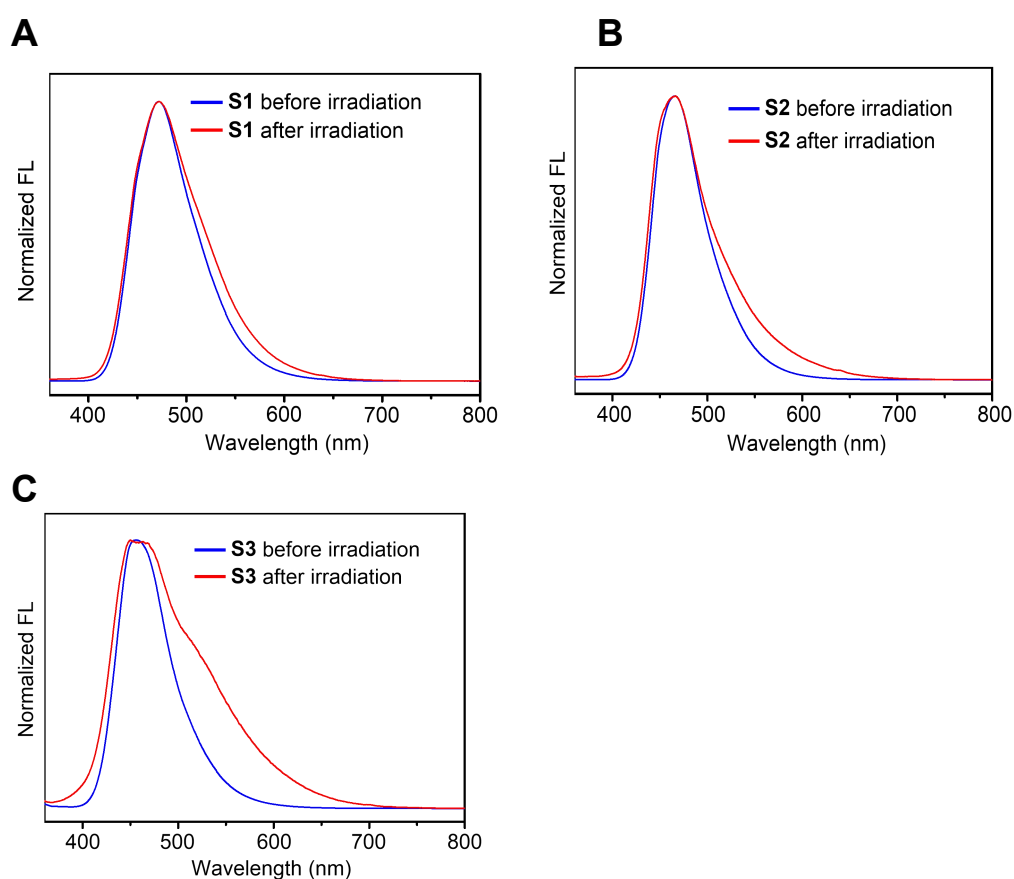


Figure 25. Normalized fluorescence spectra of **S1**, **S2**, and **S3** films (A, B, and C, respectively) before and after irradiation of L-CPL. The excitation wavelength for **S1** and **S2** were 370 nm, for **S3** was 350 nm. The films were prepared from solutions at the following concentrations: 5.0×10^{-3} M for **S1** and **S2** and 2.5×10^{-3} M for **S3**.

3.7 Conclusions

In summary, three star-shaped molecules in film were readily made optically active by CPL irradiation. The comparisons between experimental and theoretical CD spectra of the geometry-optimized models of the molecules proved that the induced chiroptical properties arise from axial chirality of the molecules around the single bonds with preferred-handed twist sense; the three molecules are proposed to have preferred-handed, three-blade propeller structures with three blades with the same handedness. Chirality amplification is considered to contribute to the formation of optically active films whose g_{CD} values were comparable with those of single-handed twisted, axially chiral molecules, indicating that the propeller conformations have high enantiomeric excesses. For the chirality amplification, molecular aggregation and ordering in the films appeared to be important. The optically active films of **S2** and **S3** exhibited efficient blue CPL with a main emission band at around 450 nm. The present work thus presented facile preparation of one-handed propeller molecules using CPL as the only source of chirality as well as the practically important properties of the optically active molecules.

3.8 Experimental

Materials. The star-shaped oligomers were available from previous work from the Hu group. Analytical data of the sample are found in the supporting information to ref. 1. Chloroform (Kanto Chemical) and (THF) (Kanto Chemical) were used as purchased. Chloroform- d_1 (99.8%, with 0.03 vol.% TMS) was obtained from Merck.

Film samples preparation. Thin-film samples were prepared by drop casting a chloroform solution of the polymers on to a quartz plate (1 cm \times 2 cm \times 0.1 cm).

CPL irradiation. CPL was generated by passing light from an Ushio Optical ModulexSX-UID500MAMQQ 500-W Hg-Xe lamp through a Gran-Taylor prism and a glass-construction Fresnel Rhomb (40 mW ($Jsec^{-1}$)). Irradiation experiments were conducted under N_2 atmosphere at ambient temperature (*ca.* 23 °C). Film surface temperature measured using a non-contact emission thermometer did not change on

irradiation and stayed at *ca.* 23 °C.

CD spectra measurements. CD spectra were obtained by averaging those recorded at four (90° interval) different film orientations (angles) with the film face positioned vertically to the incident light beam for measurement. Linear dichroism contributions were thus minimized to afford true CD spectra.

Measurements. Circular dichroism (CD) spectra were taken with a JASCO-820 spectrometer. UV-vis absorption spectra were measured on a JASCO V-570 spectrophotometer. Film temperature was measured using a Yokogawa non-contact emission thermometer 53002. IR spectra were recorded with a JASCO FT/IR-6100. NMR spectra were recorded on JEOL JMN-ECX400 spectrometers. Size exclusion chromatography (SEC) measurements were carried out using a chromatographic system consisting of a JASCO DG-980-50 degasser, a HITACHI L-7100 pump, a HITACHI L-7420 UV detector and a HITACHI L-7490 RI detector, equipped with TOSOH TSKgel G3000H HR and G6000H HR columns (30 × 0.72 (i.d.) cm) connected in series (eluent: THF, flow rate: 1.0 mL/min). Dynamic light scattering (DLS) measurements were conducted using a Nicomp 380 ZLS particle sizing system equipped with a 532 nm diode laser scattering at an angle of 90° with respect to the incident light beam was detected. Polarized optical micrographs were taken using a Nikon Eclipse E600 POL microscope. Excitation and emission spectra were taken using a JASCO FP-8500 fluorescence spectrophotometer. Circularly polarized luminescence (CPL) and nonpolarized fluorescence spectra were measured by using a dual-purpose CD and CPL spectrophotometer (J-700CPL) equipped with Stokes-Mueller matrix analysis system. CPL measurements were conducted by Prof. Takunori Harada (Oita University, Japan).

Computer Simulation. Molecular mechanics structure optimization was effected using the UNIVERSIAL⁹ force field implemented in the Discover module of the Material Studio 2.0 (Accelrys) software package with the Fletcher-Reeves¹⁰ conjugate gradient algorithm until the RMS residue went below 0.01 kcal/mol/Å. Molecular dynamic simulation was performed under a constant NVT condition in which the

numbers of atoms, volume, and thermodynamic temperature were held constant. Berendsen's thermocouple¹¹ was used for coupling to a thermal bath. The step time was 1 fs and the decay constant was 0.1 ps. Conformations obtained through MD simulation were saved in trajectory files at every 5 or 10 ps and were optimized by MM simulation.

References

1. He, X.; Chen, L.; Zhao, Y.; Chen, H.; Ng, S. C.; Wang, X.; Sun, X. Simultaneously enhancement of quantum efficiency and color purity by molecular design in star-shaped solution-processed blue emitters. *Org. Electron.* **2016**, *37*, 14-23.
2. Wang, Y.; Sakamoto, T.; Nakano, T. Molecular chirality induction to an achiral π -conjugated polymer by circularly polarized light. *Chem. Commun.* **2012**, *48* (13), 1871-1873.
3. (a) Wang, Y.; Harada, T.; Phuong, L. Q.; Kanemitsu, Y.; Nakano, T. Helix induction to polyfluorenes using circularly polarized light: chirality amplification, phase-selective induction, and anisotropic emission. *Macromolecules*, **2018**, *51* (17), 6865-6877. (b) Wang, Y.; Kanibolotsky, A. L.; Skabara, P. J.; Nakano, T. Chirality induction using circularly polarized light into a branched oligofluorene derivative in the presence of an achiral aid molecule. *Chem. Commun.* **2016**, *52* (9), 1919-1922.
4. (a) Nakano, T.; Takewaki, K.; Yade, T.; Okamoto, Y. Dibenzofulvene, a 1, 1-diphenylethylene analogue, gives a π -stacked polymer by anionic, free-radical, and cationic catalysts. *J. Am. Chem. Soc.* **2001**, *123* (37), 9182-9183; (b) Nakano, T.; Yade, T. Synthesis, structure, and photophysical and electrochemical properties of a π -stacked polymer. *J. Am. Chem. Soc.* **2003**, *125* (37), 15475-15484; (c) Hayashi, K.; Akutsu, H.; Ozaki, H.; Sawai, H. Bis (phenanthroline)-ethylenediamine conjugate displays excimer fluorescence upon binding with DNA. *Chem. Commun.* **2004**, (12), 1386-1387.
5. Pietropaolo, A.; Cozza, C.; Zhang, Z.; Nakano, T. Temperature-dependent UV absorption of biphenyl based on intra-molecular rotation investigated within a combined experimental and TD-DFT approach. *Liq. Cryst.* **2018**, 1-6.
6. (a) Feringa, B. L.; Van Delden, R. A. Absolute asymmetric synthesis: the origin, control, and amplification of chirality. *Angew. Chem., Int. Ed.* **1999**, *38* (23), 3418-3438; (b) Nakano, T. Tricks of light on helices: transformation of helical polymers by photoirradiation. *Chem. Rec.* **2014**, *14* (3), 369-385; (c) Kawasaki, T.; Sato, M.; Ishiguro, S.; Saito, T.; Morishita, Y.; Sato, I.; Nishino, H.; Inoue, Y.; Soai, K. Enantioselective synthesis of near enantiopure compound by asymmetric autocatalysis triggered by asymmetric photolysis with circularly polarized light. *J. Am. Chem. Soc.* **2005**, *127* (10), 3274-3275; (d) Kagan, H. B.; Balavoine, G.; Moradpour, A. Can circularly polarized light be used to obtain chiral compounds of high optical purity?. *J. Mol. Evol.* **1974**, *4* (1), 41-48; (e) Li, J.; Schuster, G. B.; Cheon, K. S.; Green, M. M.; Selinger, J. V. Switching a helical polymer between mirror images using circularly polarized light. *J. Am. Chem. Soc.* **2000**, *122* (11), 2603-2612.

7. (a) Rettig, W.; Zander, M. On twisted intramolecular charge transfer (TICT) states in N-aryl carbazoles. *Chem. Phys. Lett.* **1982**, *87* (3), 229-234; (b) Lifshits, L. M.; Budkina, D. S.; Singh, V.; Matveev, S. M.; Tarnovsky, A. N.; Klosterman, J. K. Solution-state photophysics of N-carbazolyl benzoate esters: dual emission and order of states in twisted push-pull chromophores. *Phys. Chem. Chem. Phys.* **2016**, *18* (39), 27671-27683.
8. Kumar, J.; Nakashima, T.; Tsumatori, H.; Mori, M.; Naito, M.; Kawai, T. Circularly polarized luminescence in supramolecular assemblies of chiral bichromophoric perylene bisimides. *Chem.-Eur. J.* **2013**, *19* (42), 14090-14097.
9. Rappé, A. K.; Casewit, C. J.; Colwell, K. S.; Goddard III, W. A.; Skiff, W. M. UFF, a full periodic table force field for molecular mechanics and molecular dynamics simulations. *J. Am. Chem. Soc.* **1992**, *114* (25), 10024-10035.
10. Fletcher, R.; Reeves, C. M. Function minimization by conjugate gradients. *Comput. J.* **1964**, *7* (2), 149-154.
11. Berendsen, H. J. C.; Postma, J. P. M.; van Gunsteren, W. F.; DiNola, A.; Haak, J. R. Molecular dynamics with coupling to an external bath. *J. Chem. Phys.* **1984**, *81* (8), 3684-3690.

Chapter 4. General Conclusions

Photo induced structural transformation of small molecule and oligomers has been investigated in this thesis. The racemization of optically active 1,1'-bi(2-naphthol) was achieved by NPL. It is surprised that polymerization of binaphthol also occurred during irradiation. Although there have been several examples about racemization of axially chiral compounds. The finding of co-occurring photo racemization and polymerization of optically active BINOL is unprecedented. Then, films of three star-shaped molecules were readily to be induced into optically active only by using irradiation of CPL without any aid molecules. CPL irradiation made the three molecules have preferred-handed, three-blade propeller structures with three blades with the same handedness.

The Photo induced structural transformation of these examples were based on the twisted-coplanar transition (TCT) of aromatic-aromatic diad structure. Though TCT has been well studied on biphenyl and fluorene-fluorene diad, this thesis further explores the applicability of this mechanism. Molecule with higher rotational barrier like binaphthol can go through such a transition. Even N-phenylcarbazole whose two different aromatic units are connected by carbon-nitrogen single bond also experienced TCT through photoexcitation. This work indicates that the TCT mechanism can be extended widely to many aromatic-aromatic diad structures, more molecules and polymers with such a structure could be modulated by light. Particularly, candidates for optically active materials whose chirality can be induced by CPL irradiation would be further expanded.

The chirality induction to polyfluorene derivatives and oligofluorene have developed CPL irradiation as an important synthesis method to obtain chiral polymers. This method has obvious advantages such as clean and inexpensive compared with any chemicals. In this thesis, the optically active star-shaped molecules induced by CPL especially **S2** exhibits strong CPL emission, which indicates that the molecules would be good candidate for practical application such as 3D display. This is a big step forward to link light-based synthesis method with practical application.

Acknowledgement

I greatly acknowledge the help of my supervisor, Prof. Dr. Tamaki Nakano. Without his patient instruction and valuable suggestion, the completion of this thesis would not have been possible.

I would like to express my heartfelt thanks to Prof. Dr. Takanori Suzuki, Prof. Dr. Takeshi Ohkuma, and Prof. Dr. Jun-ya Hasegawa who reviewed my thesis and gave me much helpful advice.

I greatly appreciate the assistance offered by Prof. Dr. Takunori Harada of Oita University, Prof. Dr. Adriana Pietropaolo of Università di Catanzaro, and Prof. Dr. Xiao 'Matthew' Hu of Nanyang Technological University for their kind collaboration.

I am greatly indebted to Dr. Yue Wang for her constant support and encouragement. Also, I wish to extend my sincere gratitude to all members of Nakano laboratory for their kind help on my research and life.

Special thanks should go to express my heartfelt gratitude to China Scholarship Council (CSC) which provide a 3.5 years scholarship for me to study in Japan.

At last, my thanks would go to my beloved family and friends for their loving consideration and great confidence in me all through these years.

Thank you all,

2019/02/26

Zhaoming Zhang

Zhao-Ming Zhang